HYDROCOASTAL

SAR/SARin Radar Altimetry for Coastal Zone and Inland Water Level

Product Validation Plan

Deliverable D2.4

Sentinel-3 and Cryosat SAR/SARin Radar Altimetry for Coastal Zone and Inland Water

ESA Contract 4000129872/20/I-DT

Project reference: HYDROCOASTAL_ESA_PVP_D2.4
Issue: 3.1b

27/09/2021

This page has been intentionally left blank

Change Record

Date	Issue	Section	Page	Comment
24/07/2020	1.0			First version
22/09/2020	2.0	various	various	Updates following ESA review. Addition of section 3.7.
26/03/2021	3.0	various	various	Addition of new sections with summary of common validation methods (§2.2 and §3.2). New section 3.10 on validation over Canadian Lakes. Minor edits and updates in other sections.
16/09/2021	3.1	various	various	Minor edits and updates following ESA's review.

Control Document

Process	Name	Date
Written by:	Mathilde Cancet, Luciana Fenoglio-Marc, Christine Gommenginger, Francisco Calafat, Jesús Gómez-Enri, Andrew Shaw, Denise Dettmering, Pierre Fabry, Nicolas Bercher, Karina Nielsen, Elena Zakharova, Joana Fernandes, Angelica Tarpanelli	26/03/2021
Checked by	David Cotton	
Approved by:		

Subject	Radar Altimetry for Coastal Zone and Inland Water Level	**Project**	HYDROCOASTAL
Author	**Organisation**	**Internal references**	
Mathilde Cancet	NOVELTIS	HYDROCOASTAL_ESA_PVP_D2.4	
Luciana Fenoglio-Marc	U Bonn		

Christine Gommenginger	NOC	
Francisco Calafat	NOC	
Jesus Gómez-Enri	U Cadiz	
Andrew Shaw	Skymat	
Denise Dettmering	TUM	
Pierre Fabry	Along Track	
Nicolas Bercher	AltHydroLab.fr	
Karina Nielsen	DTU	
Elena Zakharova	NUIM	
Joana Fernandes	U Porto	
Angelica Tarpanelli	CNR-IRPI	

	Signature	Date
For HYDROCOASTAL team		27/09/21
For ESA	Date: 2021.09.29 '11:45:08 +02'00 Digitally signed by Jérôme Benveniste	

Table of Contents

1 Introduction

1.1 The HYDROCOASTAL Project

The HYDROCOASTAL project is a project funded under the ESA EO Science for Society Programme, and aims to maximise the exploitation of SAR and SARin altimeter measurements in the coastal zone and inland waters, by evaluating and implementing new approaches to process SAR and SARin data from CryoSat-2, and SAR altimeter data from Sentinel-3A and Sentinel-3B.

One of the key objectives is to link together and better understand the interactions processes between river discharge and coastal sea level. Key outputs are global coastal zone and river discharge data sets, and assessments of these products in terms of their scientific impact.

1.2 Scope of this Report

This document is the Product Validation Plan (PVP) report for HYDROCOASTAL and it corresponds to the deliverable D2.4. of the project. The scope of this report is to describe the validation activities that will be carried out during the project.

1.3 Document Organisation

This document is organised in four main sections:

- Section 1: A short introduction defining the scope of this report.
- Section 2: The activities planned to validate the L2 products in the coastal zones (CZ).
- Section 3: The activities planned to validate the L2, L3 and L4 products in the inland waters (IW).
- Section 4: The validation activities for the new Wet and Dry Troposphere corrections.

1.4 Reference documents

HYDROCOASTAL Proposal: SAR/SARin Radar Altimetry for Coastal Zone and Inland Water Level. Proposal, January 2020.

2 Validation of the Test Datasets in different Coastal Zone Scenarios

2.1 Introduction

In this section, we describe the activities that will be carried out to validate the Test Dataset Geophysical parameters against other satellites and in situ data, in different Coastal Zone Scenarios (e.g. low lands, cliffs, fjords, cays, estuaries and man-made structures).

These validation activities include the analysis of the influence of land proximity and ground-track orientation on SAR/SARin, the analyses of the different algorithms proposed to produce the final dataset and validation against independent observations.

2.2 Summary of Methodology

Here, we present a summary of the methodology to validate the outputs of the retrackers. This method was agreed by all the teams involved in the validation of the test datasets in coastal zones.

Parameters to be validated:

- Sea Level Anomaly (SLA).
- Significant Wave Height (SWH).
- Wind Speed (U_{10}).

<u>Sea Level Anomaly (from retrackers)</u>

- Range corrections: Ionospheric, dry and wet tropospheric corrections (two WTC will be tested: from the University of Porto and ECMWF model).
- Geophysical corrections:
    - DAC: NOT APPLIED.
    - SSB: Three strategies were agreed:
        - SSB NOT APPLIED.
        - SSB = 5% of SWH (Note: the source of the SWH will be L2 enhanced product from ESA L2 product).
        - In case of retrackers giving its own SSB, a third version of SLA will be validated.
    - Tidal Model: Two global models will be tested: GOT4.10 and FES2014.
    - Ocean long period tide, solid earth tide, and 'ocean' pole tide (% of pole tide).

Water Levels (from TGs)

- DAC: NOT APPLIED.
- Tides: removed using constituents from harmonic analysis.

Data screening (Altimeter SLA & Tide Gauge Water Level (WL))

- Thresholding eliminating data beyond ±1.5 m;
- Outlier detection using the 3-sigma criterion.

Validation Metrics (Altimeter SLA & Tide Gauge WL)

- Bias;
- Pearson's correlation coefficient (r);
- Standard deviation of the differences (SDD).

Collocation criteria and extra information

- Posting rate: 20 Hz along the track segments (one time series will be created at each 20-Hz along-track position).
- Seasonal cycle and trend: NOT REMOVED from the time series as the time period of analysis is too short (2 years).
- Time-mean over the common time period of analysis REMOVED from the time series.
- Validation made along the whole track segment without any cut off for proximity to coast. Instead, rely on data flags and data screening. U Bonn and SKYMAT will be calculating distance to coast and might provide to partners.
- Collocation criteria:
    - German Bight:
        - TG time sampling: 1 minute.
        - TG time series will be built using the time of the closest measurements to the time of the altimeter data.
    - Harvest region:
        - TG time sampling: 60 minutes.
        - Assignation of the altimetry data to distance bands of a certain width, and then averaging the altimetry records falling within each band. The corresponding in situ matching value is obtained by linearly interpolating the high-frequency observations to the time of the corresponding altimetry pass.
    - Gulf of Cadiz and Strait of Gibraltar:
        - TG time sampling: 5 minutes.
        - TG time series will be built using the time of the closest measurements to the time of the altimeter data.

<u>Significant Wave Height (from retrackers, except for ALES+ for SAR retracker)</u>

A common methodology/screening was agreed regarding the data screening on altimetry and buoy SWH, with the rejection of SWH outside the interval [0 m; 15 m].

The time sampling of the wave data is region-dependent as it is directly linked with the type of instruments that are available in each region:

- German Bight and Baltic Sea: 10 minutes.
- Harvest region: from 30 to 60 minutes.
- Gulf of Cadiz and Strait of Gibraltar: from 60 minutes (smaller time samplings would be available).

For reference, we note the screening approach recommended by Saleh Abdalla (ECMWF) for the ESA CCI ECV Sea State project. This screening is applied to 1 Hz data:

- Erroneous values (negative values, zero values, SWH values > 20 m).
- Standard deviation of 20-Hz range > 0.20 m.

Validation metrics

- Bias;
- Pearson's correlation coefficient (r);
- Standard deviation of the differences (SDD)/RMSE.

Wind speed (from retrackers)

A common methodology was not agreed yet.

2.3 Validation in the German Bight/Baltic Sea region (U Bonn)

The validation activities focus on the German Bight and Baltic Sea coastal region and include the Elbe estuary. The goal is to carry out a characterization of the product performance with estimation of the data accuracy. U Bonn will perform a cross-validation analysis of the new SAR products against other altimeter products, model data and in-situ data. The study area has been used for the validation of radar altimeter data in open ocean and near the shore, see Fenoglio et al. (2015, 2019, 2020) and Dinardo et al. (2018, 2020).

The German Bight region is a mesotidal environment with varying geometry and difficult-to-couple interactions between the meteo-oceanographic and morphodynamical factors. A major similarity among the Elbe, Ems and Weser estuaries is the tidal and atmospheric forcing. Semidiurnal tides with a range of ~3–4m during spring periods are the major drivers. The tidal wave propagates up to the weirs, which are in Herbrum for the Ems, Bremen-Hemelingen for the Weser and Geesthacht for the Elbe. The distances from the mouths to the limnic parts of the estuaries are comparable: from ~30–40 km in the estuaries of Ems and Weser to ~70 km in the Elbe Estuary. The long-term river runoff of Ems, Weser and Elbe is ~80, 330, and 710 m^3/s, respectively. On the contrary, in the Baltic Sea the ocean tidal signal is very small.

A large network of fiducial reference measurements and model data are available through the German national agencies (BfG, BKG, and BSH). The water level data are from the German Federal Institute of Hydrology (BfG) database (https://www.pegelonline.wsv.de) and from BSH. Most stations are co-located with a GPS station and the ellipsoidal height of the zero marker of the tide gauge data are made available by BfG and by the Federal Agency for Cartography and Geodesy (BKG). The height of the zero marker is known for all stations above the national reference height system (NHN). The PSMSL and SONEL databases include some of them (TGBF, TGCU, TGWD, WARN, SASS and TGKI). Sixteen stations have been used to study sea level change from conventional and SAR altimetry in Fenoglio et al. (2020) and along-track SAR data were found to give rmse between 2 cm and few decimeters compared to in-situ data. The tide gauge stations available for this study (triangle) are shown together with wave station data available from BSH (square) in Figure 2.3.1.

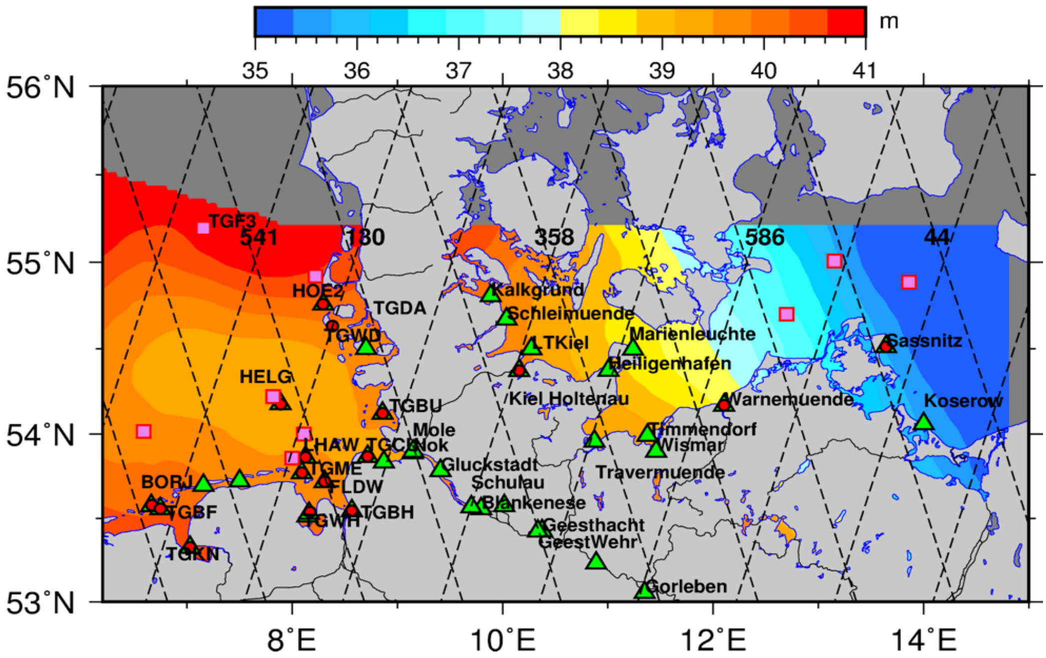

Figure 2.3.1 Region selected and in-situ data. Stations with water level (green triangle), GPS (red circle) and wave height measurements (pink square).

2.3.1 Times series of data

The altimetry-derived sea level heights above the ellipsoid WGS84 (SSHi) are obtained by applying all the environmental and selected geophysical corrections depending on the application. For the in-situ and model validation, the ocean tide correction and the Dynamic Atmospheric Correction (DAC) are not applied. The Range is corrected for the effect of ionosphere, wet and dry troposphere (Range Corrections in Eq. 2.3.1) and for the solid earth tide, load tide and for the part of the pole tide related to the solid earth (Geophysical Corrections_i in Eq. 2.3.1 below, see also Eq. 3-5 in Fenoglio-Marc et al., 2015). The sea state bias correction applied is 4.7 % of the significant wave height. The solid earth tide correction does not include the zero-frequency term, called permanent tide, thus the altimeter heights are referred to the mean tide system.

The HYDROCOASTAL altimeter-derived SSHi instantaneous time series to be compared to the uncorrected tide gauge observations will be calculated using Eq. (2.3.1):

SSHi = Altitude - Range - (Range Corrections + Geophysical Corrections_i) (2.3.1)

with Range Corrections including all the environmental corrections and Geophysical Corrections_i including all the geophysical corrections except the Dynamical Atmospheric Correction (DAC) and the ocean tide.

The TG time series will be built using the time of the closest measurements to the time of the altimeter data. The time sampling of TG data is 1 min for coastal and open sea stations, in case of gaps at the station the time lag accepted between altimetry and tide gauge data is 5 minutes. The Sea Level Height of the TG in the mean height system will be obtained from Eq. (2.3.2)

$$SSHi\_TG = \text{Water Level} + TG_{zero} \qquad (2.3.2)$$

with *Water Level* the tide gauge measurement and TG_{zero} the ellipsoidal height in the mean tide system of the reference point (zero) of the tide gauge zero. Eq. (2.3.1) and (2.3.2) allow an absolute comparison of heights, which is possible only when the GPS (red circle in Figure 2.1) and the tide gauge (green triangle) are co-located. If TG_{zero} is not available from GPS, the comparison of the sea level anomalies (SLA_i) is made considering the height anomalies of SSHi over a given time interval, which corresponds to the subtraction of a mean sea surface MSS (see Eq. 2.3.3).

SLAi = Altitude - Range - (Range Corrections + Geophysical Corrections_i) - MSS (2.3.3)

SLAi_TG = Water Level - mean(Water Level) (2.3.4)

A large part of the residual differences between SLAi and SLAi_TG arises from the difference in ocean tide at the two locations. The residuals are further reduced by applying the ocean tide correction estimated by an ocean model at each location using Eqs. (2.3.5) and (2.3.6) to compute the time series.

SLA = Altitude - Range - (Range Corrections + Geophysical Corrections_i) - MSS - ocean tide (2.3.5)

SLA_TG = Water Level - mean(Water Level) - ocean tide (2.3.6)

The two last equations are similar, but not coincident, to Eqs. (2.3.1) and (2.3.2). The difference lies in the corrections applied (pole tide related to the solid earth, no DAC, ocean tide from model at the tide gauge in Eqs. 2.3.3 and 2.3.4)

The time sampling of wave data (square in Figure 2.1) is 10 minutes, in case of gaps at the station the time lag accepted between altimetry and wave data is 30 minutes.

2.3.2 Data screening

A first screening of the altimeter data consists of rejecting data over land, inland waters and shallow water depth lower than 2 m. Secondly, we apply thresholds to SSH and SWH eliminating SSH data with departure from the mean sea surface (MSS) larger than 15 m and SWH outside the range between 0 m and 15 m. Thirdly, different outlier detection rules are applied to the sea level anomaly (SLA) and SWH parameters in coastal and in open sea separately. Standard outlier detection rule is a 3-sigma criterion. The measurements may also be filtered using the misfit parameter between the model and data waveforms if available for the given retracker. A high value of misfit indicates land contamination or a waveform corresponding to a specular surface. As the SLA in the coastal zone is normally distributed and the SWH is not, the misfit criterion is preferable for the SWH parameter (Dinardo et al., 2018).

2.3.3 Validation approaches

An along-track comparison of the data with computation of the statistics (bias, standard deviation of differences and correlation) over a selected part of the track are evaluated (Figure 2.3.2). The new SAR products will be cross-validated against other new and standard products and against ocean model data in scatterplots in open sea and coastal areas. See Figure 2.3.3 for an example of scatterplot comparing Sentinel-3A 1 Hz sea level anomalies in open sea from SAMOSA+ and SAMOSA2 (Dinardo et al., 2020). The average in bands of 200 meters of the standard deviation of sea level anomalies (STDSLA) as a function of the distance to the coast will be analyzed for altimetric products and models. One model is taken as reference and the departure between the altimeter and this model is assumed to indicate land contamination in the altimeter data.

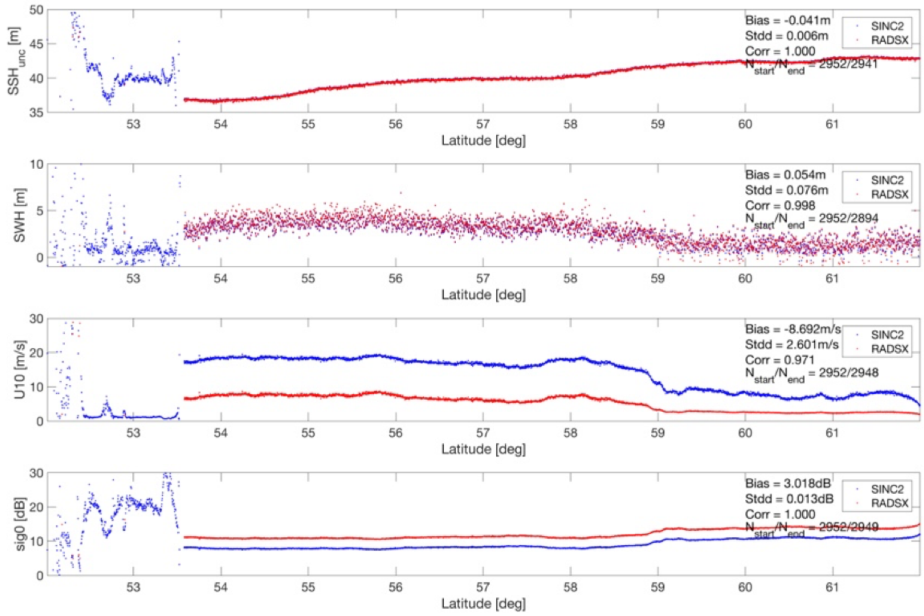

Figure 2.3.2 Along-track comparison of the CryoSat-2 geophysical parameters from different products. In this case Pseudo LRM from the RADSX database (20Hz RADS-Brown retracker, R.Scharroo personal communication) and TUDaBo database (20 Hz SINC2 retracker, Buchhaupt e al., 2018).

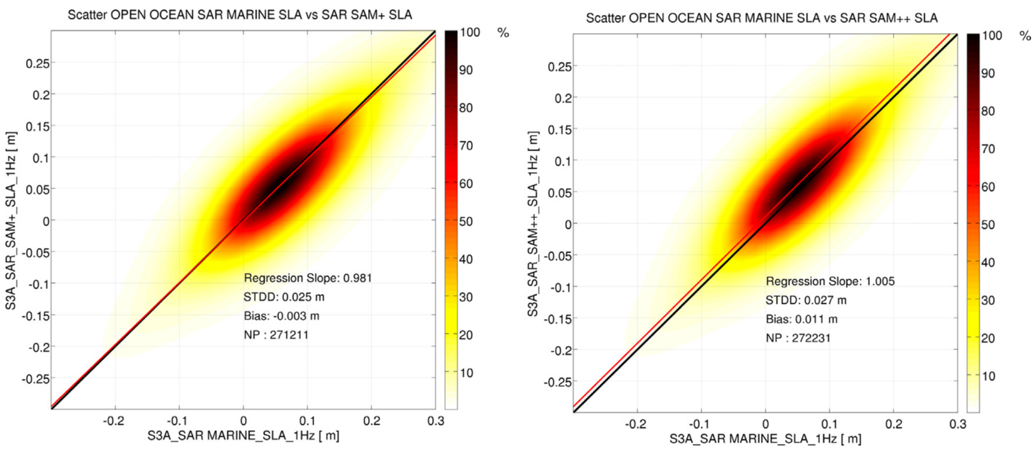

Figure 2.3.3 Scatterplots of Sentinel-3A 1 Hz sea level anomalies in open sea from SAMOSA+ and SAMOSA2 (Dinardo et al., 2020).

To investigate the precision of each single product separately, we investigate the standard deviation of SLA as a function of the SWH. An example is shown in Figure 2.3.4 for the SAR Marine and SAR SARvatore SAMOSA++ products (Dinardo et al., 2020). The quality of the altimeter data is investigated in terms of noise level, with the noise estimated as the absolute value difference between consecutive SSH measurements at 20 Hz. An example is shown in Figure 2.3.5 for the SAR SARvatore SAMOSA+ and the RDSAR TUDaBo products (Fenoglio et al., 2020). The nearest measurements at 1 Hz and 20 Hz within a selected range of distances from the tide gauge stations are selected and time-series are built. The statistics (bias, standard deviation of differences (STDD)) is computed from the two time-series. Time-series of altimetry data are constructed along the ground-track by assigning the altimetry data to distance bands of a certain width, and then averaging the altimetry records falling within each band. The pairs altimetry and tide gauge are compared using the metrics above applied to sea level anomalies. The ocean tide is corrected using a tide model at both locations. Alternatively, the ocean tide harmonic components at the in-situ stations are computed by harmonic analysis or extracted from the published values. The metrics are computed with and without the sea bias altimeter correction of a defined percentage of the significant wave height.

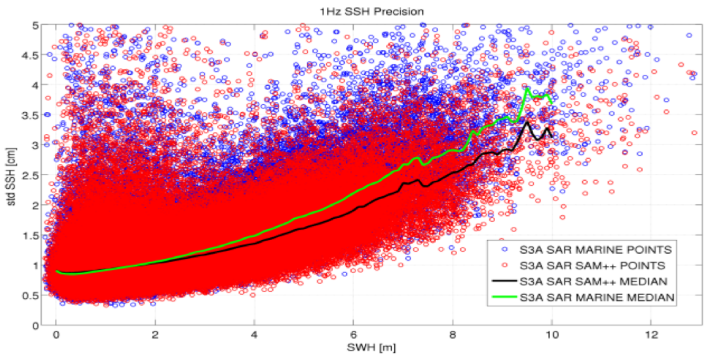

Figure 2.3.4 Standard deviation of SLA as a function of the SWH for the SAR MarineSAMOSA2 and SAR SARvatore SAMOSA++ products

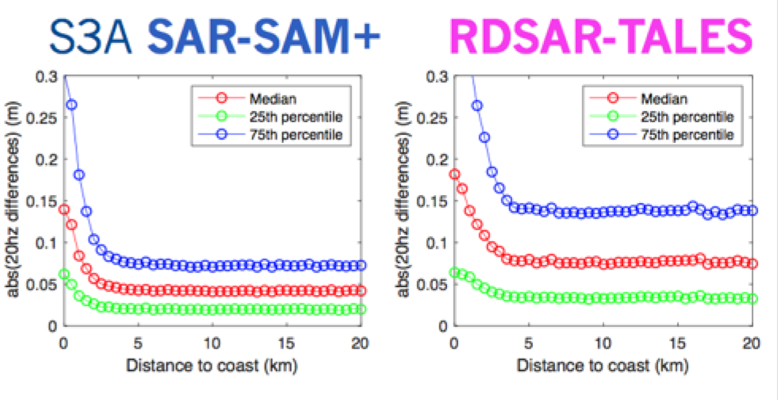

Figure 2.3.5 Noise level of SSH measurements at 20 Hz for SAR SARvatore SAMOSA+ and RDSAR TUDaBo

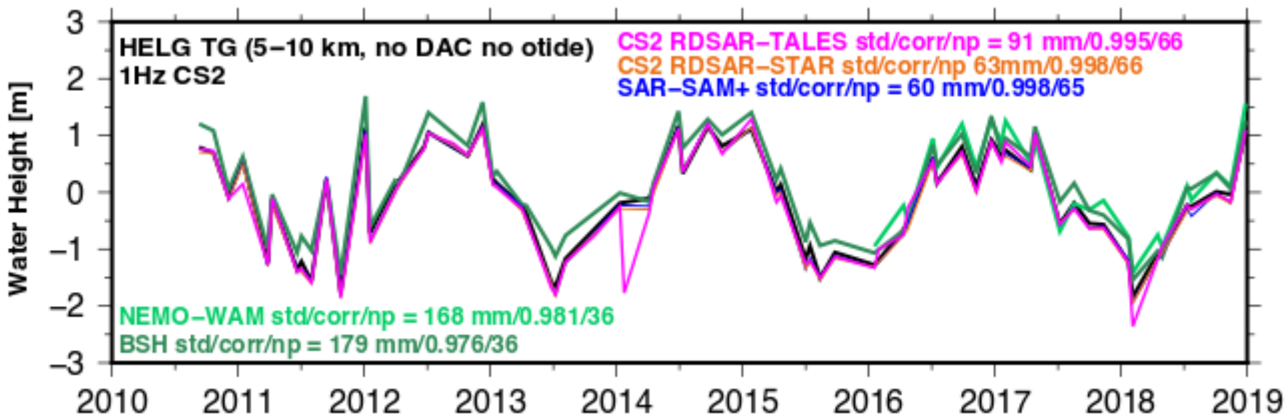

Figure 2.3.6 Sea level anomalies of CryoSat-2 at tide gauge Helgoland uncorrected for ocean tide and DAC.

2.4 Validation in the Harvest region (NOC)

The validation activities will focus on the Harvest region on the West coast of the United States.

The region is of interest for validation because of the large number of high-quality in situ measurements of sea level, wave height and wind speed from tide gauges and moored wave buoys in the region. Data from large network of fiducial reference measurements are available freely through the Global Sea Level Observing System (GLOSS) tide gauge network (available via the University of Hawaii Sea Level Centre, UHSLC; https://uhslc.soest.hawaii.edu/), and the US National Data Buoy Center (NDBC; www.ndbc.noaa.gov). The GPS data will be obtained from SONEL (https://www.sonel.org).

In addition, the region offers several other characteristics that make this a particularly interesting and challenging site to test innovative algorithms for coastal SAR processing such as NOC's Specialised COastal OPerator for SAR waveforms (SCOOP-SAR):

- the west-facing Pacific coastline is famously subject to energetic swell and high sea states in winter, providing a wide range of conditions in a relatively short period (1 year minimum). The dense (relatively) network of wave buoys provide in situ measurements of the full set of wind and sea state parameters (e.g., wave period, and in some cases, directional wave spectra) to support validation of retrieved sea state both offshore and inshore.
- the general orientation of the coastline (SE-NW) offers a variety of oblique approaches to the satellite tracks
- the nature of the coastal land mass (coastal mountains, urban areas, inland water) present many opportunities for contamination of ocean echoes from inland targets.
- the presence of a string of coastal islands.

Figure 2.4.1 shows the area where satellite data will be acquired and processed, the location of in situ stations, the Cryosat-2 SAR mode acquisition box and the ground-tracks of the Sentinel-3A and 3B altimeters.

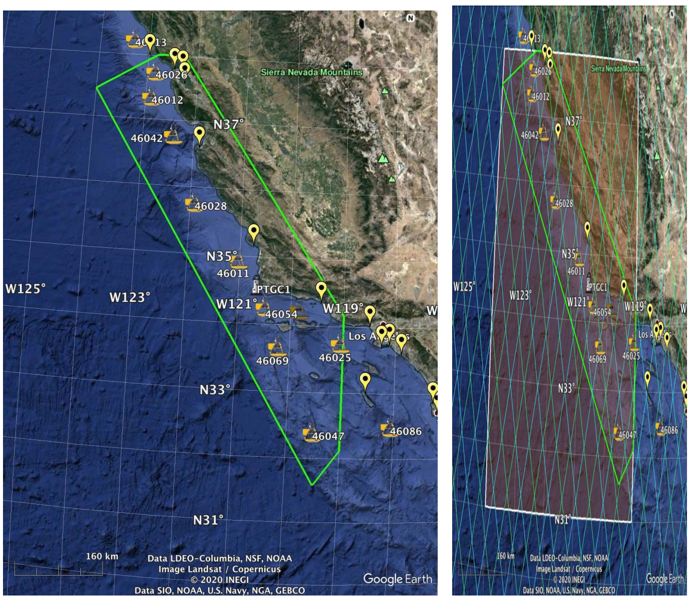

Figure 2.4.1 (left) Harvest validation test site (green polygon) showing the location of coastal tide gauges (yellow/black markers) and moored wind and wave buoys. (right) Same with Cryosat-2 Harvest SAR mode box and Sentinel-3A/B STM ground tracks (blue/green lines).

2.4.1 Assessing improvements in data recovery and quality

Improving the recovery and quality of SAR altimeter data close to land is the main objective of advanced coastal SAR retrackers. The new coastal SAR datasets will be evaluated using standard diagnostic tools used in coastal altimetry. These will be applied to sea surface height (and derivative products, e.g SSHA) and significant wave height. Assessment of wind speed will be attempted but may raise issues linked to the dependence of Sigma0 on wind speed close to land. The coastal altimetry assessment metrics and diagnostic tools to be used include:

- % valid data recovery with distance to coast
- Median/Std with distance to coast
- Misfit
- Std v significant wave height

The assessment will NOT include power density spectra (e.g. of SSH or SWH) since those may not provide reliable results over such a small region.

2.4.2 Validation against in-situ data

The SAR altimeter measurements of SSH, SWH and wind speed will be validated against in situ data.

Validation of SAR altimeter wind and wave data will use standard match-up methods with moored buoy data from available NDBC stations (https://www.ndbc.noaa.gov/). NDBC wind and wave data are 20-minute averages reported hourly or half-hourly. Maximum separation time between the altimeter and in situ wind and wave data will thus be 30 minutes, nominally. In the case of SWH, we will remove values larger than 15 m. Note that the validation of SAR wind speed will only be tentative given the added complexity of validating coastal winds.

In the case of SSH, the validation will be conducted against tide gauges. Comparisons will be done in terms of absolute heights (i.e., ellipsoidal heights) wherever there is a geodetic tie between the TG and a nearby GPS station, otherwise the comparison will be based on sea level anomalies (SLAs).

The altimetric SSHs will be computed by subtracting the corrected range from the altitude, where the former is defined as the range corrected for ionospheric and tropospheric (wet and dry) path delays as well as sea state bias (SSB). The corrections across regions and algorithms will be harmonized to facilitate comparisons with other algorithms and other regions (i.e. German Bight/Baltic and Cadiz/Gibraltar).

In designing a validation strategy for SSH, it is important to recognize that generally altimetry measurements are not collocated with the tide gauges. This spatial separation will necessarily lead to differences in sea levels between the two types of measurements, and the ocean tide can be a major contributor to such differences. Hence, here the comparison will be conducted for detided time series, noting that while tide gauges only sense the ocean tide and the ocean pole tide, altimeter measurements are also influenced by the solid earth tide, the load tide, and the solid earth pole tide, and so these tidal contributions will all be removed from the altimetry data. With this in mind, the altimetric SSHs will be computed according to:

SSH = Altitude - Corrected_Range - Geophysical_Corrections   (2.4.1)

where Geophysical_Corrections denote the solid earth, pole, load, and ocean tides. Note that we do not apply the DAC.

The SLAs are computed by subtracting the mean sea surface (MSS) from the SSHs:

SLA = SSH - MSS   (2.4.2)

As part of the screening of the altimetry data, we will remove values of SLAs (in both the SSH and the SLA) beyond 1.5 m and beyond 3 standard deviations.

The relative sea levels from the tide gauges are expressed with respect to the ellipsoid using the following equation (Andersen et al., 2018):

$$SSH\_TG = Water\_Level + TG_{zero} - Ocean\_Tide - (MSS_{TG} - MSS) \quad (2.4.3)$$

where Water_Level is the relative sea level as observed by the tide gauge, TG_{zero} is the ellipsoidal height in the mean tide system of the reference point of the tide gauge zero, Ocean_Tide denotes the ocean tide (including the ocean pole tide), and MSS_{TG} is the mean sea surface at the TG location. The term within parenthesis on the right-hand side of Eq. (2.4.3) accounts for differences in the mean sea surface due to spatial separation between the altimetry and the tide gauge data, which can appear as biases in the absolute validation even if there are not any true biases. MSS_{TG} is known exactly from the TG data if the TG benchmark is connected to a GPS (ignoring observational errors in the TG and the GPS), but MSS is precisely the quantity that we aim to evaluate. This means that, in practice, the term within parenthesis cannot be estimated exactly. Here, a multi-mission MSS product will be used to quantify (MSS_{TG} - MSS), acknowledging that there may be errors near the coast.

The ocean tide at the TG can be obtained from either harmonic analysis of the TG data or from a tide model. Harmonic analysis generally provides a much better prediction of the tide than a numerical model, particularly at the coast where local tidal effects can be difficult to model. Hence, this is the approach that we will follow.

We anticipate that at most TG sites it will not be possible to obtain ellipsoidal heights due to the unavailability of GPS data, and so this validation will focus on SLAs. The SLAs from the TG (SLA_Tg) will be obtained by removing the time mean from SSH_TG.

In the Harvest region, TG data are hourly averages. This means that the maximum temporal separation between the in-situ and altimeter measurements, in the absence of data gaps, will be 30 min for the TGs. If gaps are present, we will still enforce a maximum separation of 30 min.

To obtain in-situ-altimetry comparison pairs, we will follow the approach that we have successfully used in previous validation activities (Calafat et al., 2017; Passaro et al., 2018; Bouffard et al., 2018). Briefly, this approach consists of averaging the altimetry records falling within a predetermined distance from the TG. The corresponding in situ matching value is then obtained by linearly interpolating the high-frequency TG observations to the time of the corresponding altimetry pass. Here, interpolating in time is preferred to simply selecting the closest point, particularly when comparing with TGs, since sea levels can vary significantly over a span of 30 minutes. Once matchup datasets are available, we will use standard quantitative statistical quantities to evaluate the quality of the new satellite altimeter data (bias, std, regression). These will be compared with similar quantities obtained with matchup datasets based on the content of the operational altimeter products.

2.5 Validation in the Gulf of Cadiz and Strait of Gibraltar regions (U Cadiz)

2.5.1 Study areas

The Gulf of Cadiz (Southwest Spain) has one of the main tributaries in Spain, the Guadalquivir River and the Doñana National Park wetlands on its right bank, close to its mouth on the Atlantic coast. Another tributary is the Tinto-Odiel System on the left of the Park. Past and present altimetry data have been validated in this area using *in situ* tide gauges deployed and managed by Puertos del Estado (www.puertos.es): Huelva station (in the mouth of the Tinto-Odiel System), Bonanza station (located in the estuary mouth of the Guadalquivir River), and Tarifa station (Strait of Gibraltar). The location of the study areas in the Iberian Peninsula is shown in Figure 2.5.1a. The location of the S3A/B tracks and the tide gauges (Huelva and Bonanza: Gulf of Cadiz) is given in Figure 2.5.1.b; the same for the Strait of Gibraltar (Tarifa station and tracks) is in Figure 2.5.1c. The CryoSat-2 tracks are not shown here.

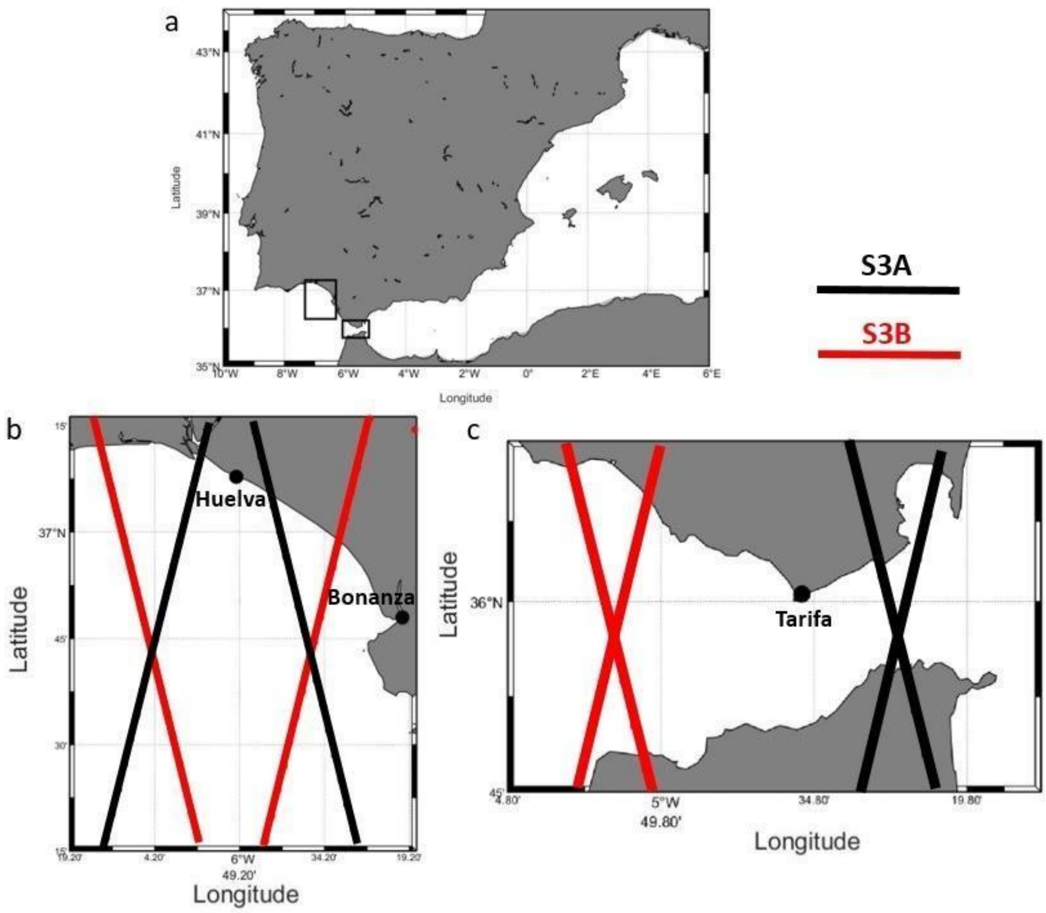

Figure 2.5.1 The Gulf of Cadiz and the Strait of Gibraltar in the Iberian Peninsula (Fig. 2.5.1.a). S3A/B tracks and TG stations in the Gulf of Cadiz (Huelva and Bonanza: Fig. 2.5.1.b) and in the Strait of Gibraltar (Tarifa: Fig. 2.5.1c).

The Huelva tide gauge station is located in the eastern shelf of the Gulf of Cadiz, Southwest of the Iberian Peninsula. Tides are mainly mesotidal, with amplitudes above 1 m. The Gulf of Cadiz surface circulation is characterized by a strong seasonality that is linked to the offshore circulation (Peliz et al., 2007). García-Lafuente et al. (2006) proposed the existence of a mesoscale cyclonic cell over the eastern continental shelf during spring-summer, its northern part being a warm coastal countercurrent (Stevenson, 1977; Relvas and Barton, 2002). This countercurrent is generally replaced by an eastward flowing current during autumn and winter (Criado-Aldeanueva et al., 2009). More recent studies (Garel et al., 2016) suggest that the onset of this countercurrent is a common feature over the year and does not show a seasonal behaviour. The Guadalquivir River also plays an important role in the eastern Gulf of Cadiz surface circulation. Sporadic but heavy freshwater discharges might contribute to the sea level at different time-scales as previously noted by Laiz et al. (2013) and Gómez-Enri et al. (2015; 2018).

The study area has also been used in the past for the validation of conventional pulse-limited and SAR-mode radar altimeter data near the shore. Gómez-Enri et al. (2012) and Laiz et al. (2013) used weekly gridded maps of SLA from AVISO (Archiving, Validation and Interpretation of Satellite data in Oceanography) to validate SLA time series at different time scales, finding high and significant correlations (r > 0.85) with *in situ* tide gauge sea level data at monthly time scales. As mentioned before, Gómez-Enri et al. (2018) validated SLA time series from the CryoSat-2 SIRAL altimeter, in SAR mode, using the Huelva tide gauge. The authors analyzed along-track data with an along-track spatial resolution of 20 Hz, obtaining rmse of 6.4 – 8.5 cm in the 5 – 20 km segment respect to the coast. Furthermore, these values increased towards the coast, ranging from 8.5 to 29.3 cm in the 0 – 5 km segment. More recently, Aldarias et al. (2020) validated 2.3 years of Sentinel-3A 80-Hz sea level data (SARvatore-GPOD and SAMOSA+ (Dinardo et al., 2018) retracker) at Huelva TG station. They found accurate S3A sea level data (rmse < 10 cm) at the [2.5 - 20] km distances to the coast for the two tracks analyzed.

The Strait of Gibraltar is the choke point between the Atlantic Ocean and the Mediterranean Sea and controls the water exchanges between both water masses. The Strait of Gibraltar has been thoroughly described in the past from different points of view. Lacombe and Richez, 1982; Bryden and Kinder, 1991, analyzed the surface flux of Atlantic water toward the East being compensated by a western flux of Mediterranean deeper, saltier, and warmer water.

From an altimetric point of view, (Fukumori et al., 2007; Menemenlis et al., 2007) analyzed the sea level difference between the Atlantic Ocean and the Mediterranean Sea near the strait using Topex/Poseidon tracks. However, they only used along-track altimeter data at 1-Hz interval (about 6 km along the ground track) in regions deeper than 1000 m at distances greater than 150 km from the eastern and western sides of the Strait. They pointed out the lack of accurate altimeter data for shallower regions. More recently, Envisat RA-2 (18 Hz) and SARAL AltiKa (40 Hz) SLA were validated in the Strait using the Tarifa TG station obtaining rmse values between 12 – 14 cm (Envisat RA-2) and between 8 and 10 cm (SARAL AltiKa) within the first 30 km from the coast (Gómez-Enri et al., 2016). A few works are in progress on coastal applications using accurate altimeter data for a better knowledge of the hydrodynamic processes in the Strait (Gómez-Enri et al., 2019).

2.5.2 Times series of data

The HYDROCOASTAL altimeter-derived SLA time series will be estimated using Eq. (2.5.1):

SLA_Retracker(n) = Altitude - Range(n) - (Range Corrections + Geophysical Corrections) - MSS (2.5.1)

where *n* corresponds to the number of retrackers used in coastal zones; *Orbit* (or Altitude) is the distance between the satellite's centre of mass and the reference surface (ellipsoid WGS84). *Range(n)* is the retracked distance between the instrument and the mean reflected surface obtained from the *n* retrackers. *Range corrections* include the dry and wet tropospheric effect obtained from the University of Porto and ECMWF models, the ionospheric correction provided by the Global Ionospheric Maps (GIM) of the Jet Propulsion Laboratory, and the Dynamic Atmospheric Correction (DAC) provided by AVISO+/CNES. The *Geophysical corrections* include the ocean equilibrium tide, the ocean long period, the ocean load tide, the solid earth tide, and the pole tide. The *Mean Sea Surface* used will be surface available in the output product.

The Sea State Bias correction (*SSB*) will not be available in most of the retrackers. In order to get a first approximation of this correction, a parametric approach will be made by estimating the best fit (in terms of the statistical approach selected) between *SLA_Retracker(n)* and *SLA_TG*, when SSB values ranging between 0% (no correction) and 10% of the SWH. Preliminary analysis made with S3A/B in Huelva and Tarifa (using the SARvatore-GPOD and SAMOSA+ (Dinardo et al, 2018) retracker) gave the results shown in Table 2.5.1. The percentage of SWH shown in the table (used as a first approximation of the SSB correction) gave the smaller rmse (see subsection 2.3.4 for details) between altimeter-derived SLA and ground-truth stations.

Table 2.5.1. Percentage of SWH to compute the SSB correction (as a first approximation) for the tracks analysed (S3A and B) at the two TG stations. Ocean-Land / Land-Ocean means the transition of the track segment.

Coasts	Huelva	Tarifa
S3A # (Ocean-Land)	4%	7%
S3A # (Land-Ocean)	4%	7%
S3B # (Ocean-Land)	5%	6%
S3B # (Land-Ocean)	7%	8%

The TG time series will be built using the time of the closest measurements to the time of the altimeter data. The temporal difference between altimeter and TG data is below 2.5 min. The Sea Levels will be obtained following Eq. (2.5.2):

$$SLA\_TG = \text{Water Level} - \text{Tide Prediction} - DAC \quad (2.5.2)$$

where *Water Level* is the sea level measurement; the Tide Prediction will be calculated from the tide gauges data with a classical harmonic analysis (Pawlowicz et al., 2002). *DAC* from AVISO+/CNES will be estimated by bilinear interpolation in space to the position of the TG station, and linear interpolation in time to the time of the instrument measurements.

2.5.3 Data screening

First, a data screening will be used to remove outliers: 1) the values outside the range: [-1.5, 1.5] m and 2) the values outside the median ± 3 σ (standard deviation). In the second step, the temporal mean of the time series will be eliminated to obtain the anomalies.

2.5.4 Statistical approaches

The altimeter-derived time series (Figure 2.5.2) will be validated with the SLA_TG using two statistical parameters, namely, the r coefficient and the rmse, as in previous works (Fenoglio-Marc et al., 2015; Passaro et al., 2016; Dinardo et al., 2018; Gómez-Enri et al., 2018; Aldarias et al., 2020; among others). The validation will be focused on the along-track segments shown in Figure 2.5.1 for S3A/B and the set of tracks for CryoSat-2, for the *n* retrackers used in the coastal zones. The dry/wet tropospheric corrections from UPorto will be also assessed for each retracker (Figure 2.5.2). The percentage of valid cycles in the track segments selected will be also computed.

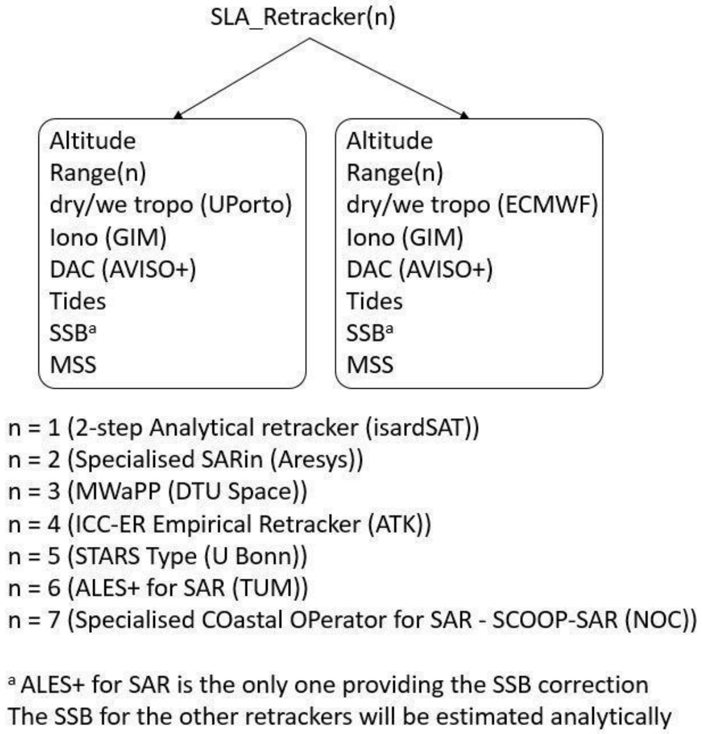

Figure 2.5.2 Schematic representation of the altimeter-derived time series with the corrections and the selected retrackers.

2.6 Influence of land proximity and angle of approach (SatOC/SKYMAT)

The performance of Sentinel-3 and CryoSat-2 SAR/SARin radar altimetry are examined by investigating their angle of approach towards the coastline. The performance of different re-trackers is assessed in terms of noise and data loss for each satellite mission. A range of different coastline types are selected to represent various coastal physical features as well as having a wide variety of orientation angles approaching the coastline. Specifically, five selected regions reflecting different coastline types are considered: the Gulf of Cádiz, German Bight and Baltic, a mixture of relatively flat terrain, and Harvest and Straits of Gibraltar with higher cliffs.

The angle of approach to the coast is computed by calculating the separation angle between the direction of the satellite track and the direction of the gradient using the coastal proximity parameter (Cipollini, 2011). This method is described in more detail in the SCOOP Product Validation Report (PVR), D2.5, Section 4.4. In this study, the separation angle dependency is assessed at 15-degree divisions and binned at 1 km intervals as a function of distance to the coast in terms of data lost close to the coast (see example Figure 2.6.1). Here, the uncorrected sea surface height (USSH(n)) is calculated from Orbit minus Range(n), where n is the number of re-trackers. No other corrections are applied. The noise is defined as successive differences of high frequency (20 Hz) USSH(n) observations along each of the tracks (Passaro et al. 2014). This also allows us to calculate the USSH(n) noise as a function of the angle of approach to the coast for each re-tracker and satellite mission for comparisons. A baseline ESA product will be used as a standard in order to compare the re-trackers for noise and data loss. The analysis of the angle of approach associated with USSH noise and data loss to the coast will use the median filter, 25 and 75 percentiles as indicators for each re-tracker(n) per satellite mission per region. This methodology is repeated for the significant wave height (SWH(n)) observations.

2.6.1 Data Screening / Filtering

A high resolution landmask will be created and applied to the satellite observations for each of the defined regions using the GMT software where the Global Self-consistent, Hierarchical, High-resolution Shorelines (GSHHS) dataset is used. Any USSH(n) values outside the median ± 3 σ (standard deviation) will be removed. The misfit parameter will also be applied.

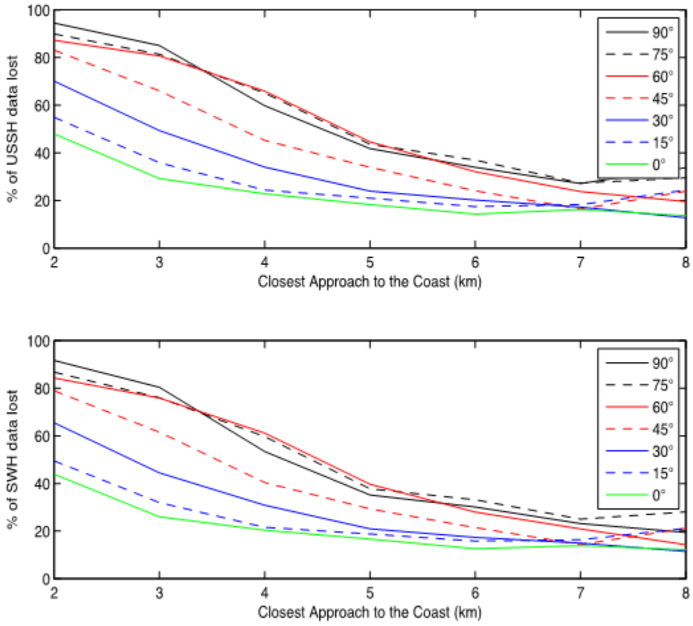

Figure 2.6.1 The percentage of the CryoSat-2 SAR Phase 2 data rejected when applying a misfit threshold of 3 from USSH and SWH parameter fields as a function of the angle of approach and distance to the coastline for the North East Atlantic region for 2012 to 2013 where 0° and 90° represents normal and parallel to the coast, respectively (SCOOP PVR, D2.5, Section 4.4)

3 Validation of the Test Datasets in different Inland Water Scenarios

3.1 Introduction

In this section, we describe the activities that will be carried out to validate the test dataset and geophysical parameters against other satellites and in situ data, in different Inland Water Scenarios (e.g. low lands, hilly areas/valleys, man-made structures, estuaries).

These validation activities include the analysis of the influence of land proximity and ground-track orientation on SAR/SARin, analysis of retracking algorithms, analyses of the different algorithms proposed to produce the final datasets of water level (L3) and river discharge (L4) and the validation against gauging data.

3.2 Summary of Methodology

This section introduces the quality indicators to be used for the sake of the validation of Water Level (L3) and River Discharge (L4) time series. Table 3.2 below lists the common measures agreed to be implemented by all partners as well as additional measures specific to individual teams.

Table 3.2 Summary of statistical measure employed for validation of L2, L3 and L4 data

Team	Area	Validated Product	Processing Level	Statistical Measure
Common statistical measures				
All partners	All areas	Water Level	L3 outputs	Relative: SD, MAD, corr Absolute: RMSE, Mean
All partners	All areas	River Discharge	L4 outputs	RMSE, NRMSE, corr, NSE
Additional statistical measures				
U Bonn	Rhine and Elbe	Retrackers	L2 (SAR and SARin) -> time series (L3)	RMSE, corr, offset
DGFI/TUM	All test areas	L3 methodology, retrackers	L3 (L4)	RMSE, NSE, offset, corr

ATK	Over areas that are covered by an updated Water Mask produced by ALONG-TRACK SAS from S1 images.	Ground Track orientation	L1	water fraction (WFR)
AHL	Amazon	Retrackers via L3	L3 (L2)	Temporal: SLR, Teff
DTU Env	Amur, Yangtze, Zambezi	Retrackers, L3 methodology	L3, L2	RMSE, corr, ME, AE
NUIM	Ob, Rhine, Mississippi	Discharge, Retrackers	L3	RMSE, Corr, bias, NRMSE, NSE
CNR-IRPI	Po, Mississippi, Rhine	Retrackers, Discharge Algorithm	L3, L4	Mean, SD, KGE index
DTU Space	Wollaston and Reindeer lakes	Retrackers	L3	Corr, RMSE, MAD
U Porto	Danube River/ Caspian, Amazon, ...	Corrections WTC, DTC	L2 corrections	

3.2.1 Level 2 and 3 Inland Water Level Products

The evaluation of the different retracking algorithms will mainly be performed through validation of the water level time series (L3). Validation of the L2 water levels may be done by the individual teams.

The validation of L3 data will **make use of in situ data in order to derive error time series** and then vertical validation indicators from the error time series. The **common validation metrics agreed to be used** are specified in table 3.2 and defined in section 3.2.4. Table 3.2 also recaps specific measures to use by individual teams.

In the validation, the focus will be on the relative change of the water level rather than the absolute water level.

Validation of L3 data will also be used to assess L2 retrackers performance.

There will also be an assessment of the different approaches to generating L3 products from L2.

3.2.2 Level 4 Inland Water Discharge Products

The objective of the L4 product assessment is to compare different methodologies for generating river discharge products. It will focus on four rivers (Rhine, Ob, Po and Mississippi).

L4 products will not be used to compare different L2 retracker performance.

The River Discharge correctness is estimated by statistical indicators such as root mean square error (RMSE) and normalized RMSE (NRMSE), Nash-Sutcliffe model Efficiency coefficient (NSE), Kling-Gupta efficiency (KGE), and more qualitative indicators based on water balance realism (Budyko framework, e.g., Berghuijs et al, 2014), as well as delay propagation error.

3.2.3 Description of Accuracy and precision indicators (L3, L4)

The indicators described below apply to a series of errors (ε) values computed as the difference of data derived from altimetry (level, discharge) minus reference data.

Mean $\mu\varepsilon$, Standard Deviation $\sigma\varepsilon$ (SD) and Root Mean Square Error (RMSE) of error ε are defined as:

$$\mu_\varepsilon = \frac{1}{N}\sum_{n=0}^{N}\varepsilon(n) \;\; ; \;\; \sigma_\varepsilon^2 = \frac{1}{N-1}\sum_{n=0}^{N}\left[\varepsilon(n)-\mu_\varepsilon\right]^2 \;\; ; \;\; RMS_\varepsilon = \left[\frac{1}{N}\sum_{n=0}^{N}\varepsilon^2(n)\right]^{\frac{1}{2}} \qquad (3.2.1)$$

Remarks:

- $\sigma\varepsilon$ is the square-root of unbiased Variance estimator;
- Generally speaking, RMSE(x) can be expressed as a combination of both the Mean and the Standard Deviation of x:

$$RMS_x^2 = \mu_x^2 + \frac{N-1}{N}\sigma_x^2 \qquad (3.2.2)$$

MAD (Median Absolute Deviation) is a robust measure of the variability of a univariate sample of data. For an error data ε (ε1, ε2, ..., εn), the MAD is defined as the median of the absolute deviations from the data's median:

$$MAD(\varepsilon) = median(|\varepsilon(n) - median(\varepsilon)|) \qquad (3.2.3)$$

that is, starting with the residuals (deviations) from the data's median, the MAD is the median of their absolute values.

Correlation coefficient

The correlation coefficient is given by

$$\rho = \frac{\boldsymbol{COV(X,Y)}}{\boldsymbol{\sigma_X \sigma_y}} \qquad (3.2.4)$$

Here COV is the covariance where $X$and Yrepresent the altimetry and in situ water levels at the times where the altimetry data is provided and σ_X and $\sigma_Y$are the standard deviation terms of the altimetry and in situ water levels.

3.2.3.1 Description of Discharge indicators (L4)

The traditional approach within the hydrological modelling community to validate river discharge model predictions are to quantify the deviation from in situ observations using statistical indicators derived from model-data error time series, for instance root-mean-square-error (RMSE), relative volume error (ratio between the mean of predicted and observed discharge), and most commonly probably the Nash-Sutcliffe model efficiency coefficient (Nash & Sutcliffe, 1970):

$$NSE=1-\frac{\sum_{t=1}^{T}\left(Q_o^{\,t}-Q_m^{\,t}\right)^2}{\sum_{t=1}^{T}\left(Q_o^{\,t}-mean(Q_t)\right)^2} \qquad (3.2.5)$$

NSE is the sum of squared error normalized by the variance of the observed data. A value of 1 indicates the time-series of observed (Qo) and modelled (Qm) discharge are identical. A value equal or below 0 means the variance of the model error is equal or larger than the variance of the observations, implying that the mean of the observations would be a better estimate than the modelled data. A recent developed performance indicator with similar behaviour is the Kling-Gupta efficiency [Gupta2009], which is summarizing the similarity between two time-series x and y in terms of mean value (m), standard deviation (s), and correlation (r):

$$KGE=1-\sqrt{\left(1-m_x/m_y\right)^2+\left(1-s_x/s_y\right)^2+\left(1-r_{x,y}\right)^2} \qquad (3.2.6)$$

KGE is also varying from minus infinity to 1. The advantage of KGE compared to NSE is that the three components can be explicitly extracted and used to identify reasons for poor model results.

3.3 Validation on the Rhine and Elbe rivers (U Bonn)

Validation activities focus on the Rhine and the Elbe rivers. The two regions are of interest for validation because of the large network of fiducial reference measurements available through the German national agencies (BfG, BKG). The location of the *in-situ* measurements is shown in Figure 3.3.1 for the Elbe Estuary and Figure 3.3.2 for the river Rhine. Stations from the Netherlands (Rijkswaterstaat) will be considered for the River Rhine. A set of in-situ stations near to the altimeter virtual stations will be selected.

Water level time series derived by retracking will be compared to a set of external water level time series in order to assess their accuracy and to evaluate the impact of the new processing techniques. As quality indicators, metrics based on correlation and root mean square errors (RMSE) will be used. For the Sentinel-3 repeat mission, a virtual point and a polygon are defined for each in-situ station. The altimeter measurements falling inside the polygon within a chosen distance from the virtual point are considered and screened out in the post-processing in case the moving standard deviation between three consecutive measurements is higher than 20 cm (Dinardo, 2020) and an average per pass is computed. The error assigned to the averaged altimeter height is the standard deviation of the averaged data, or the standard deviation read from the data products, if only one measurement is used. For the CryoSat-2 mission instead the averaged altimeter measurements at the virtual point locations will be evaluated by comparison with other altimeter products and in-situ data. Their combination in time-series will be attempted accounting for the slope of the river.

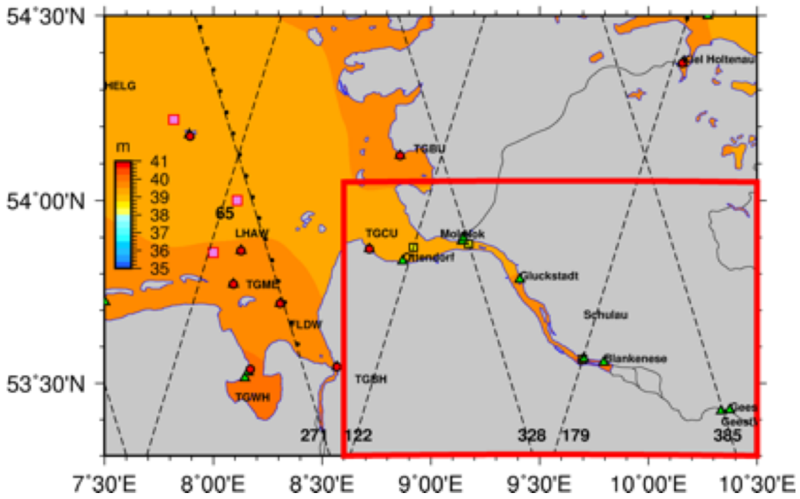

Figure 3.3.1 Elbe Estuary with in-situ stations and Sentinel-3A ground tracks

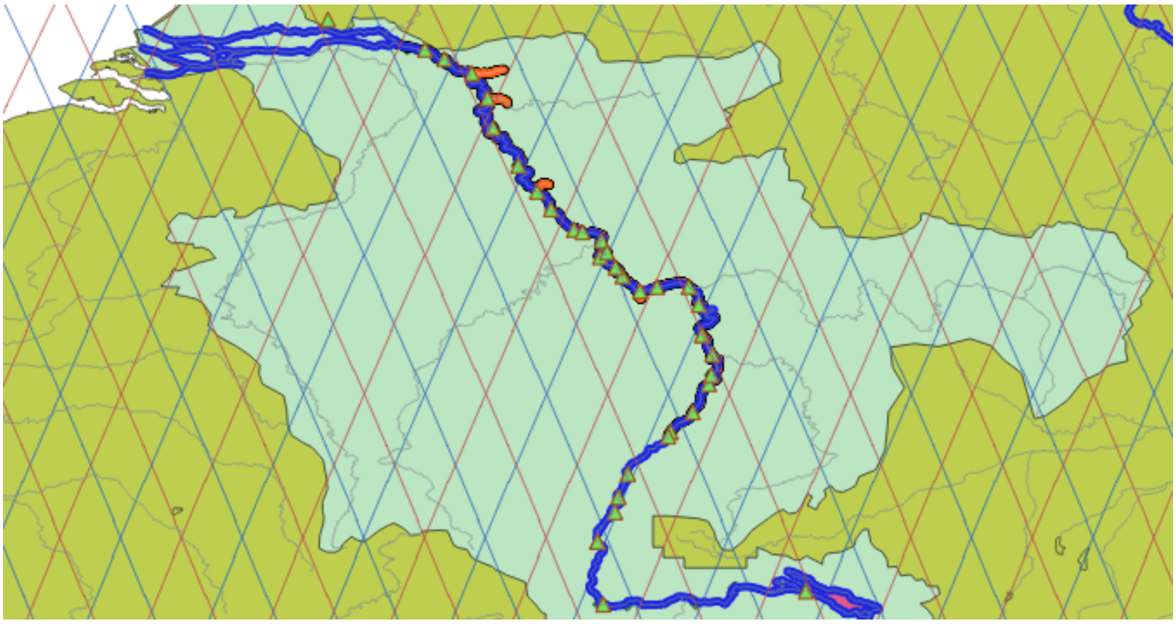

Figure 3.3.2 River Rhine with level gauge location (green triangle) and Sentinel-3A/3B (red/blue) tracks.

3.4 Validation of Water Level Time Series (DGFI/TUM)

In order to perform an independent assessment of inland water level time series derived from the different dataset providers, an inter-comparison as well as a validation in different globally distributed sites will be performed (by an institution not providing inland water level time series itself).

The HYDROCOASTAL inland water level time series (L3 data) will be compared to each other and to a set of external water level time series in order to assess their accuracy and to evaluate the impact of the new processing techniques. Moreover, the impact of different tropospheric corrections (standard and provided within this project will be assessed. As quality indicators, we will use correlation, root mean square errors (RMSE), Nash-Sutcliffe-Efficiency (NSE), as well as offset analyses.

The external data sources used for comparison will be the following:

- in situ gauging data from different sources;
- Altimetry-derived water level time series as provided by DAHITI (https://dahiti.dgfi.tum.de; Schwatke et al., 2015). Depending on the availability of data, single-mission time series from Sentinel-3 as well as from other missions will be used. In addition, in case of larger lakes multi-mission time series are used;
- Lake level time series derived from surface area time series based on optical images (Schwatke et al., 2019) combined with (sparse) stage data following a hypsometry approach (e.g. Busker et al., 2019, Schwatke et al., 2020).

The validation will be performed on a set of different inland water bodies (rivers, lakes, and reservoirs) of different sizes and characteristics, globally distributed all over the continents. This will provide an overview on the quality of the new time series depending on target characteristics. Moreover, the impact of dedicated SAR processing (developed within HYDROCOASTAL) will be visible through the direct comparison with Sentinel-3 DAHITI time series, which are treated in DAHITI just like classical LRM missions (i.e., based on standard retracking (with empirical ITR retracker) of multi-looked L1B waveforms).

3.5 WFRWF[1] approach, influence of ground-track orientation and water fraction (ATK)

Land proximity and ground-track orientation are acceptable approaches in simple coastal cases (not in fjords, not in the case of small islands, small rivers, etc.). It has been noticed that these concepts provide both a degraded and an ambiguous representation of the altimeter footprint content, which is therefore inappropriate in most inland water cases (especially flooded plains, meandering river path, complicated topology of the water body). Instead, an analysis of the Water Content in the Footprint based on water masks will better correlate to the geophysics of the scene, and be more predictive and easier to handle. Such work has been initially developed in the frame of the SHAPE project (Fabry et al. 2015, 2016), cf. Figure 3.5.1.

The concept of water fraction ratio (WFR) brings a more complete and elegant response to the need of testing "the influence of ground track orientation relative to coastline and riverbanks and land proximity" as it provides much more information and can provide a way of editing the altimetry records in these scenarios.

WFR may be an interesting asset only when it is associated with updated water masks (High Resolution Water Masks obtained from co-dated imagery w.r.t. to the altimetry acquisition date). In this project the budget allocated to the production of High-Resolution Water Masks is limited, and the idea is to prove the benefit of the WFR concept. WFR will be provided wherever updated Water Masks are produced by ALONG-TRACK SAS. The WFR will be provided as a separate netCDF file or as an update of the ICCER output file for areas that are covered by one of the 5 masks that will be produced.

The Validation team will then be in position to test the benefit of such additional field in their validation exercise and also at the time of producing the water level time series.

[1] Water Fraction Ration, Water content in Footprint

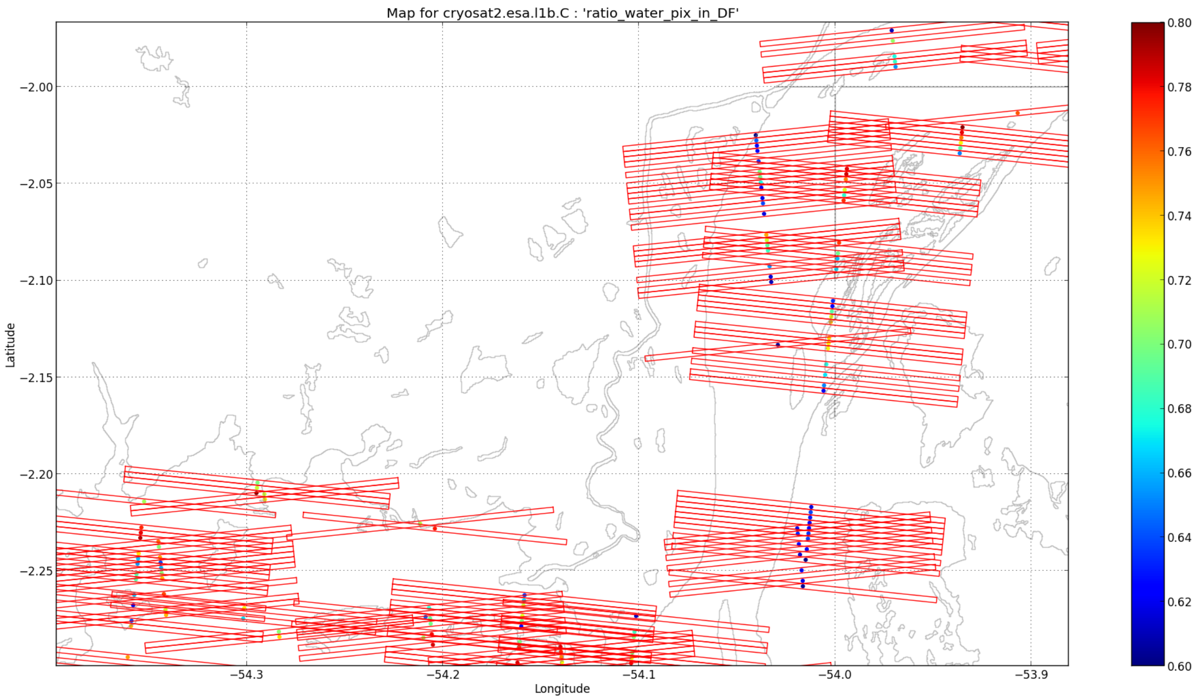

Figure 3.5.1 CryoSat-2 Baseline-C, Beam-Doppler limited footprints (20Hz records) over the Amazon downstream together with SWBD water masks on background and a central dot whose color indicates the water fraction (WFR) in each footprint (for the 60-80% interval here). (Extracted from Fabry et al., 2016, ATK.)

Currently (and in the illustration above) a coarse method is used to determine the Beam-Doppler limited footprint extent. The footprints are computed, at each record, from the longitude, latitude, tracker range, satellite altitude and velocity found in CryoSat-2 L1B files and system parameters (3dB antenna beam-width, burst PRF). As depicted in the figure above, the Beam-Doppler limited footprints are derived from several points along the beam limits in the local Earth-tangential plane (ENU: East North-Up). This makes it possible to compute, for each footprint, the footprint area (FA) as well as the water area (WA) at the intersection with the water masks. We then define the water fraction as:

$$WFR = WA / FA. \quad (3.5.1)$$

The footprint size relates to the satellite velocity Vsat, its range to ground *h*, the central wavelength λ, and the burst *PRF*:

$$\Delta x = h.\frac{\lambda}{2V_{sat}}.\frac{PRF}{64} \qquad (3.5.2)$$

An approximation of the across-track beam size *D* is:

$$D = h.\tan(\theta_B + \frac{\upsilon}{2}) - h.\tan(\theta_B - \frac{\upsilon}{2} \qquad (3.5.3)$$

where θ_B is the 3dB across-track antenna aperture (roughly 1.2 deg) and υ is the boresight angle (0 degree as the attitude angles have not been considered in this early version of the footprint computation module).

A finer method will probably be available for this project. This method fully accounts for the available attitude angles provided in the products. It consists in projecting the antenna boresight to its “exact” location at the surface (tracker range related) of the ellipsoidal Earth (WGS84). The along-track limits are then determined in the Earth-tangential plane (ENU: East North-Up) centered on this “exact” footprint centre using Eq. 3.5.2 while the across-track are now obtained from projecting the antenna across-track aperture to the ellipsoidal Earth. Improved WFR are expected upon the condition of using an up to date water mask.

3.6 Validation against in situ data over the Amazon Basin (AHL)

Part of the TDS validation will be implemented over the Amazon basin for tens of virtual stations over rivers. This process leads to statistically significant results because of the large number of locations and measurements that can be validated.

Ideally speaking, gauging stations with vertical spirit leveling will be involved. In this case, quality indicators will include RMSE and mean error. However, for stations without trusted vertical spirit leveling RMSE and mean error will not be computed and the validation will be limited to Standard Deviation (relative validation) and the MAD. Other quality indicators (not related to vertical measurement but to temporal sampling of the altimetry-based river water level time series) are the Sampling Loss Rate (SLR, in %) and the effective revisit period (Teff, in days). For L3 RWL time series, SLR indicates the ratio of lost measurements w.r.t. the nominal number of measurements (=1 per pass over the river at revisited crossing place).

The absolute vertical spirit leveling is available for almost one hundred of gauging stations (Kosuth et al., 2006), some other gauging stations might be used without spirit leveling. Figure 3.6.1 provides an overview of the leveled gauging data available vs. satellite coverage (CryoSat-2 mode masks and Sentinel-3A tracks).

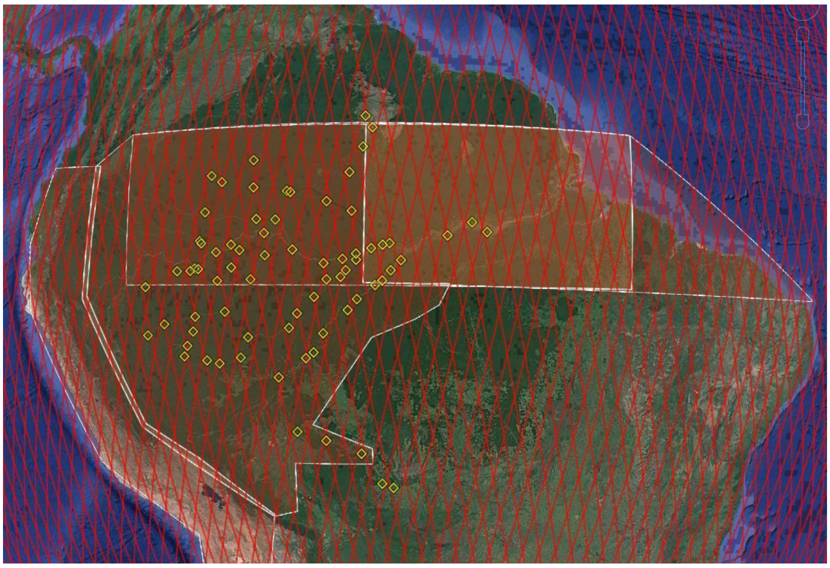

Figure 3.6.1 Map for TDS Validation of CryoSat-2 SARM & SARINM and Sentinel-3 SARM data against in situ gauging data over the Amazon basin. The Polygons represent the various CryoSat-2 SARM and SARIn Mode masks, red lines are Sentinel-3A tracks and yellow diamonds are the location of ANA gauging stations with absolute spirit leveling (96 stations), several hundreds of unleveled stations also exist and can be used to perform relative validation (i.e., no absolute bias computed).

In situ data availability over the Amazon basin is very good, however not always complete and sometimes erroneous. The database that will be used is based on ANA data with some corrections applied to fix known errors (e.g., arbitrary shifts by 1 metre). Data are usually available within a delay ranging from 1 to 12 months (typically 6 months) depending on the gauging station. As a consequence, it is likely that too recent data will not be eligible for validation.

3.6.1 Description of additional temporal indicators

The temporal indicators described below provide means to understand the temporal efficiency of Altimetry-derived time series (of water levels) at level-3 (L3). They are independent from the vertical validation of the Altimetric data themselves.

Effective Sampling Period, noted Teff, is the mean temporal period of water level time series, defined as follows:

$$T_{\text{eff}} = \frac{T_{Sat}.N_{Sat}}{N_{\text{eff}}} \qquad (3.6.1)$$

With Tsat being the satellite orbit repeat period, Nsat the number of nominal measurements, and Neff the number of acquired measurements..
Remark: Teff is greater (degraded cases) than, or equal (nominal case) to, Tsat.

Sampling Loss Rate (SLR), noted ηeff, is, for water level time series, the ratio of the number of measurements lost by the “L1 to L3” Altimetry System (may occur for many reasons like orbit drifts, inoperative instrument, degraded quality of the acquisitions, outlier measurement being rejected, etc.) to the nominal number of measurements. For a single nominal track crossing a water body, it is linked to the Effective Sampling Period by the following relation:

$$\eta_{eff} = 1 - N_{sat}/N_{eff} = 1 - T_{sat}/T_{eff} \qquad (3.6.2)$$

with Nsat and Neff being, respectively, the number of nominal measurements and the number of acquired measurements; Tsat and Teff being, respectively, the nominal sampling period and the Effective Sampling Period.

For instance, Sentinel-3A products should be characterised by Tsat = 27 days (13.5 measurement per year) at a single-track Virtual Station. If it is to provide only 6.75 measurements per year, then its sampling loss rate would be 50%.

In the case of a multiple tracks Virtual Station, the representative value is calculated as the weighted mean of the ηeff from each track.

3.7 Validation against in situ data for Amur, Yangtze and Zambezi (DTU)

The test dataset water surface elevation (WSE) will be validated against in-situ station observations for three continental-scale river systems, the Amur, the Yangtze and the Zambezi. In all 3 basins, previous studies have evaluated availability and performance of CryoSat-2 and Sentinel-3 water surface elevation (Jiang et al., 2017, Jiang et al., 2019, Jiang et al., 2020, Kittel et al., 2020). The test dataset WSE will be validated by calculating standard performance statistics for the different WSE datasets, including root mean squared error, correlation coefficient, mean absolute error and mean error. Table 3.7.1 lists stations in the Amur/Songhua system, available data types and data periods. Figure 3.7.1 shows a corresponding map.

Table 3.7.1. Available in-situ validation stations in the Amur

Station Name	**Data type (WL=water level, Q=discharge)**	**In-situ data availability period**
Harbin	WL + Q	2007-2014
Jiamusi	WL + Q	2007-2014
Yilan	WL + Q	2007-2014
Tonghe	WL + Q	2007-2014
Luobei	WL	2010-2012
Jiayin	WL	2010-2012
Fuyuan	WL	2010-2012

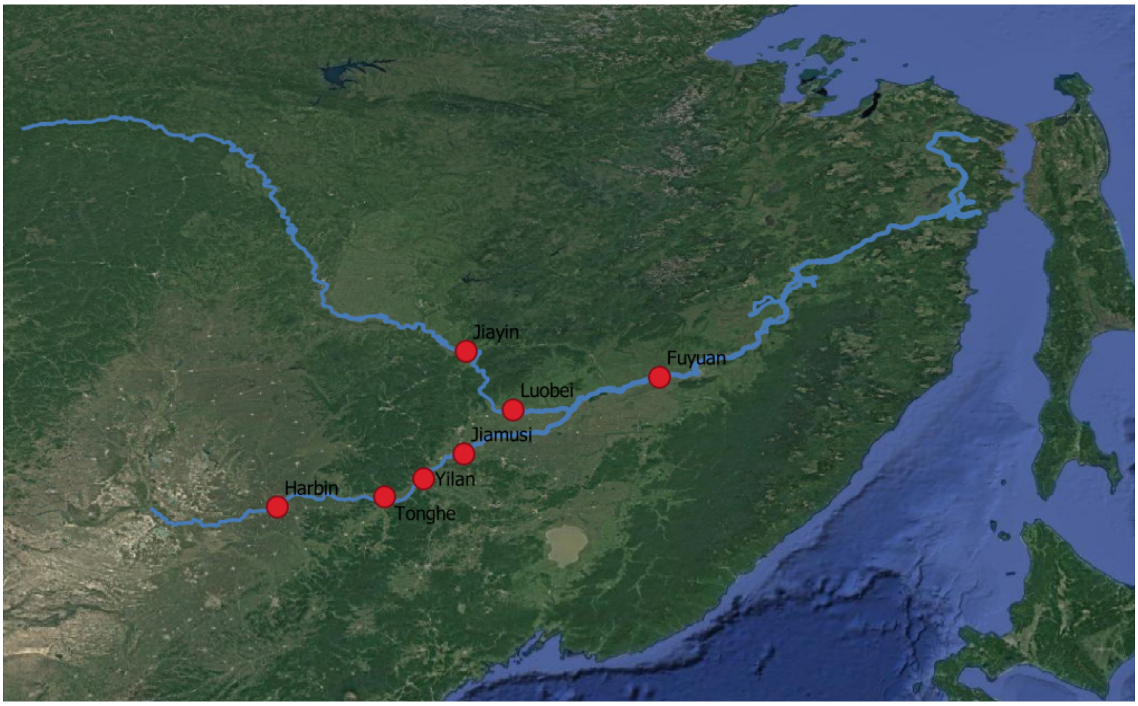

Figure 3.7.1 Available in-situ stations in the Amur-Songhua

Table 3.7.2 lists the stations in the Yangtze system, available data types and data periods. Figure 3.7.2 shows a corresponding map.

Table 3.7.2. Available in-situ validation stations in the Yangtze

Station Name	**Data type (WL=water level, Q=discharge)**	**In-situ data availability period**
Zhimenda	WL + Q	2016-19
Gangtuo3	WL + Q	2016-19
Shigu	WL + Q	2016-19
Panzhihua2	WL + Q	2016-19
Longjie3	WL	2016-19
Huatan	WL	2016-19
Yibin	WL	2016-19
Lizhuang	WL	2016-19
Luzhou3	WL	2016-19
Hejiang	WL	2016-19
Zhutuo3	WL + Q	2016-19
Cuntan	WL + Q	2016-19
Changshou2	WL	2016-19
Qingxichang3	WL	2016-19
Zhongxian	WL	2016-19
Wanxian2	WL	2016-19
Fengjie	WL	2016-19
Wushan	WL	2016-19
Badong3	WL	2016-19
Maoping2	WL	2016-19
Sandouping2	WL	2016-19
Huanglingmiao	WL + Q	2016-19
Yicang	WL + Q	2016-19
Zhicheng	WL + Q	2016-19
Majiadian	WL	2010-14,16-19
Chenjiawa	WL	2016-19

Shashi	WL + Q	2016-19
Haoxue	WL	2016-19
Xinchang2	WL	2016-19
Shishou	WL	2016-19
Tiaoxiankou	WL	2016-19
Jianli	WL + Q	2016-19
Luoshan	WL + Q	2010-14,16-19
Hankou	WL	2010-14,16-19
Huangshigang	WL	2016-19
Matouzhen	WL	2010-14,16-19
Jiujiang	WL	2010-14,16-19
Anqing	WL	2010-14,16-19
Datong	WL + Q	2010-14,16-19

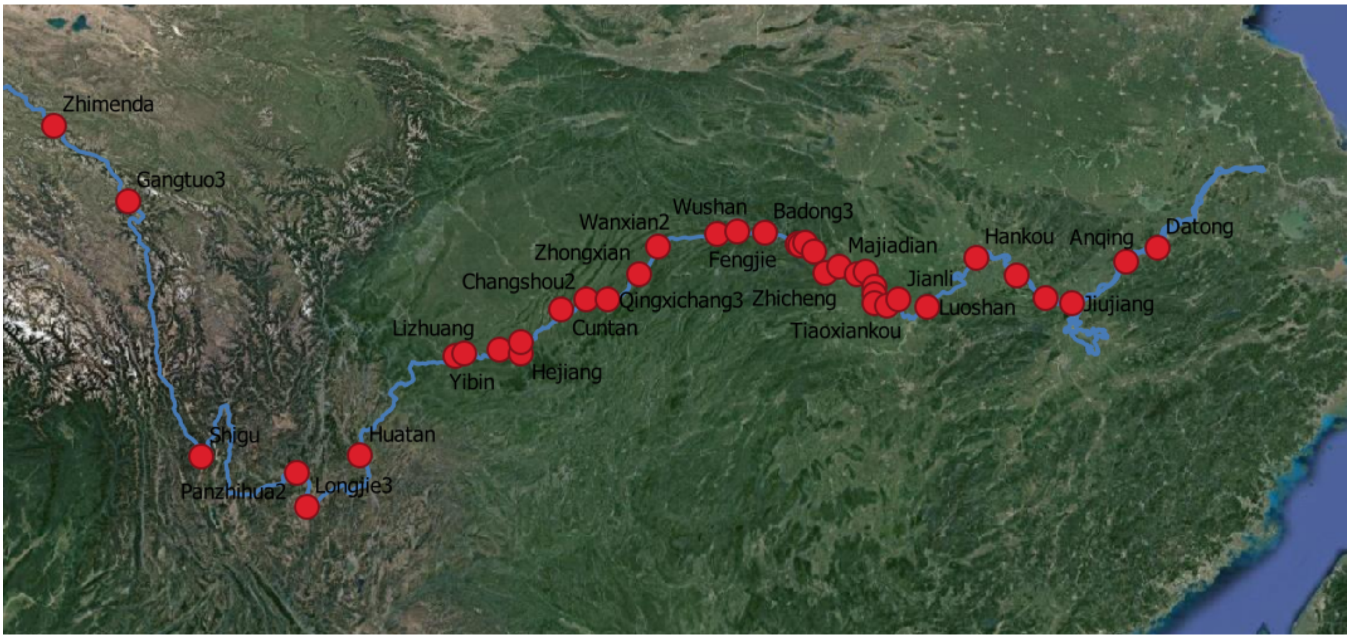

Figure 3.7.2 Available in-situ stations in the Yangtze

Table 3.7.3 lists stations in the Zambezi system, available data types and data periods. Figure 3.7.3 shows a corresponding map.

Table 3.7.3. Available in-situ validation stations in the Zambezi

Station Name	Data type (WL=water level, Q=discharge)	In-situ data availability period
Chavuma	WL + Q	2015-present
Watopa	WL + Q	2017-present
Lukulu	WL	2017-present
Kalabo	WL + Q	2017-present
Matongo Platform	WL	1956-present
Senanga	WL	1970-present
Ngonye Falls	WL + Q	2005-present
Sesheke	WL	1960-present
Nanas Farm	WL + Q	2013-present
Victoria Falls	WL + Q	1924-present
Kalomo	WL + Q	2006-present
Gwayi	WL + Q	1999-present
Ume	WL + Q	2008-present
Sanyati	WL + Q	2017-present

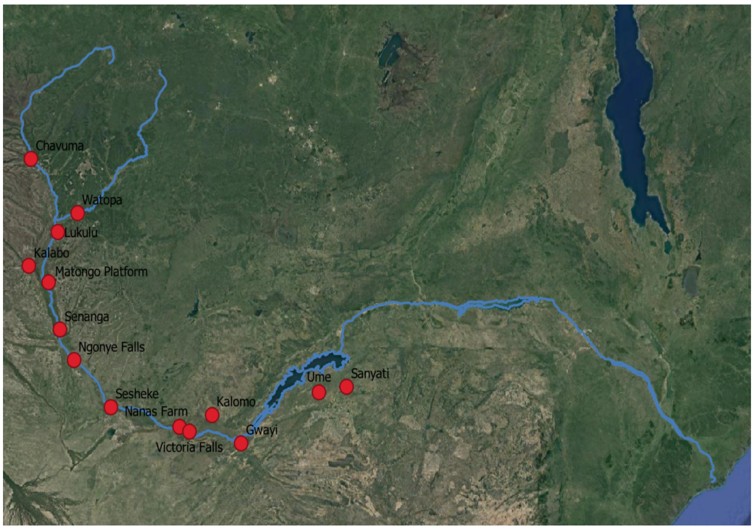

Figure 3.7.3 Available in-situ stations in the Zambezi

3.8 Validation against in situ data for Ob and Rhine Rivers (NUIM)

The altimetry-derived water (L3) and river discharge (L4) products will be validated against in situ observations of water level and discharge on one large Arctic River (the Ob) and one middle-size temporal climate river (the Rhine). In situ observations for the water level for the Ob River are available at Salekhard station for 2009-2020, while the discharge will be reconstructed using equations developed in Kouraev et al. (2004) and Zakharova et al. (2020) and based on information provided by Russian Hydrometeorological Service for earlier years. Special attention will be paid for the accuracy of the retrievals during ice season.

In situ observations of the water level for the Rhine River are available from automatic gauging stations located within the German territory. Several locations will be selected for validation of the water level retrievals to address an effect of the fluvial morphology (Figure 3.8.1(a)). The in-situ measurements are of 15-min frequency allowing for evaluation of effect of sub-daily level variability during the flood rise.

The river discharge will be calculated by three methods (rating curves, Bjerklie equation and Manning equation) and the accuracy of each method will be evaluated against in situ observations at annual scale and for a specific hydrological phase using common statistics:

- root mean square error (RMSE), absolute and normalised on average discharge, computed for study period
- correlation coefficient;
- bias
- Nash-Sutcilffe Efficiency (NSE)

To address the problem of the satellite sampling frequency and accuracy of altimetric freshwater fluxes estimates, monthly and annual water flow will be calculated from the altimetric retrievals. These values will be compared with similar quantities derived from daily in situ data.

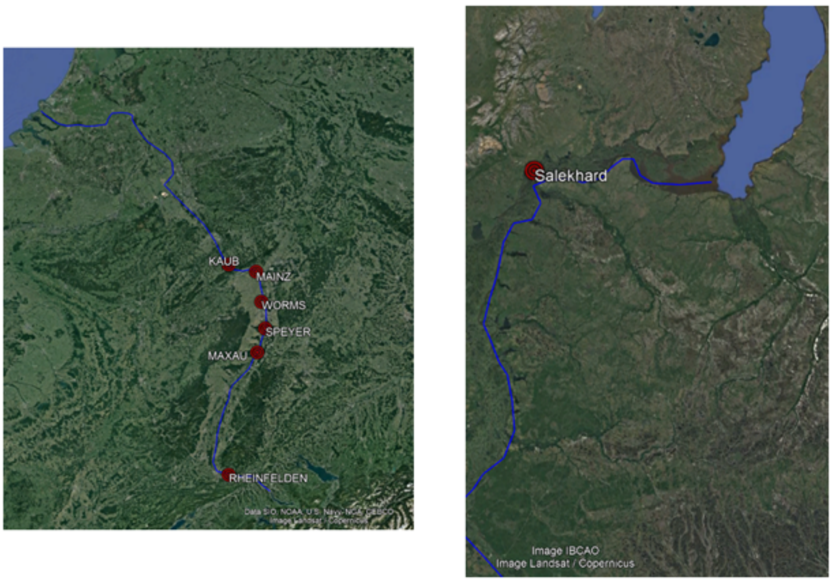

a) b)

Figure 3.8.1 Location of discharge gauging stations on the Rhine (a) and Ob (b) Rivers.

3.9 Validation against in situ data for Po and Mississippi Rivers (CNR-IRPI)

The altimetry-derived water level (L3 product) and the simulated river discharge (L4 product) validation will be performed through the comparison of the products with in situ observations recorded at specific gauged stations. Specifically, thanks to the numerous gauged stations dislocated along the two selected rivers, Po and Mississippi (see Figure 3.9.1), the validation procedure will be applied to sites not used for developing and implementing the algorithm for the river discharge estimation based on the merging between altimetry and imaging sensor. In such a way, an independent dataset of sites, not used in the previous steps, will be tested to ensure the quality of the algorithm.

The validation will be carried out at different scales, daily and monthly, and through both a direct comparison of temporal series and the duration-curve, that shows the percentage of time that flow in a stream (or water level) is likely to equal or exceed some specified values of interest.

Several metrics will be produced for water level and river discharge validation, considering in situ measurements. For the water levels, the following performance metrics will be produced:

- coefficient of correlation, *R*, to quantify the temporal agreement between in situ and satellite water level;
- root mean square error, *RMSE*, to quantify the difference in magnitude between in situ and satellite water level;
- mean and standard deviation of the error to identify the statistical metrics.

The metrics will be evaluated in terms of relative heights to avoid influence of difference in datum (often unknown for the in situ measurements) or the distance between the virtual station and the gauged station. The relative heights will be computed by removing the long-term mean of both the temporal series.

For the river discharge, the above water level metrics of *R* and *RMSE* will be used, along with:

- Normalized *RMSE*, *NRMSE*, defined as the *RMSE*/$\underline{Q_{obs}}$, where $\underline{Q_{obs}}$ is the mean of the observed discharge;
- Nash-Sutcliffe efficiency index, a measure of goodness-of-fit with respect to the observed mean;
- the Kling-Gupta efficiency index, that provides direct assessment of three aspects of discharge time series, namely shape, timing and variability.

An exercise of validation of river discharge will also be carried out at three sites along the Rhine in order to compare the approach with those used from NUIM.

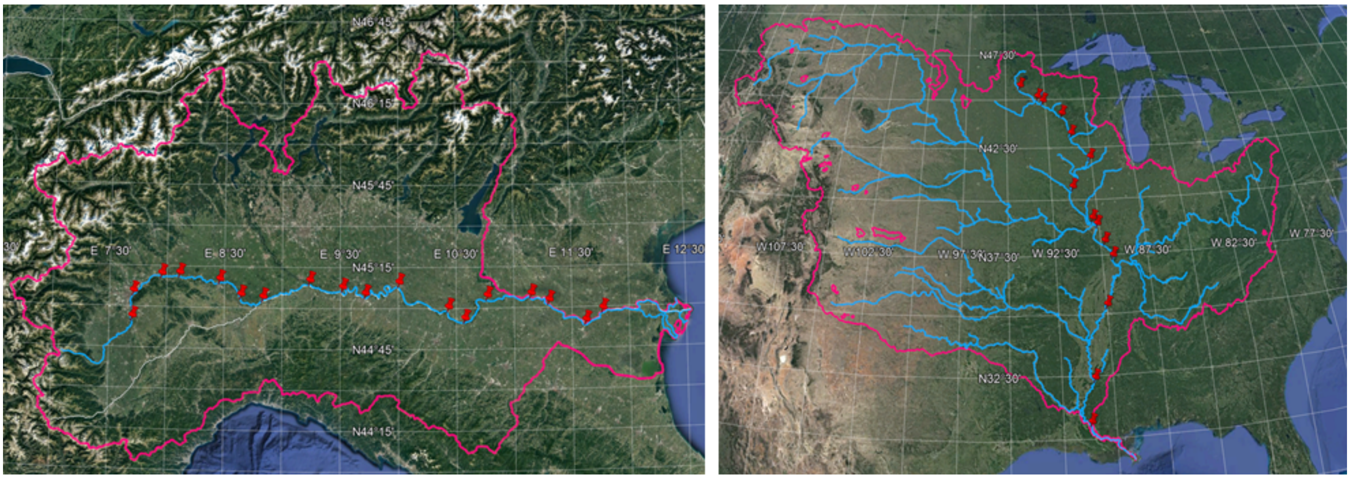

Figure 3.9.1 Location of discharge gauging stations on the Po (left) and Mississippi (right) Rivers.

3.10 Validation against in situ data over the Canadian Lakes Reindeer and Wollaston (DTU)

Here the L2 and L3 products will be validated against in situ level data. These lakes are frozen in the winter which will allow for an evaluation of the retracker performance when lake ice is present. We will perform both an along-track analysis to estimate the number of outliers and an evaluation of the time series, where the summary measures root mean square error and Pearson correlation are estimated. To avoid bias issues due to the difference between the vertical reference of the gauge and altimetry data we will focus on evaluation the relative water level variations.

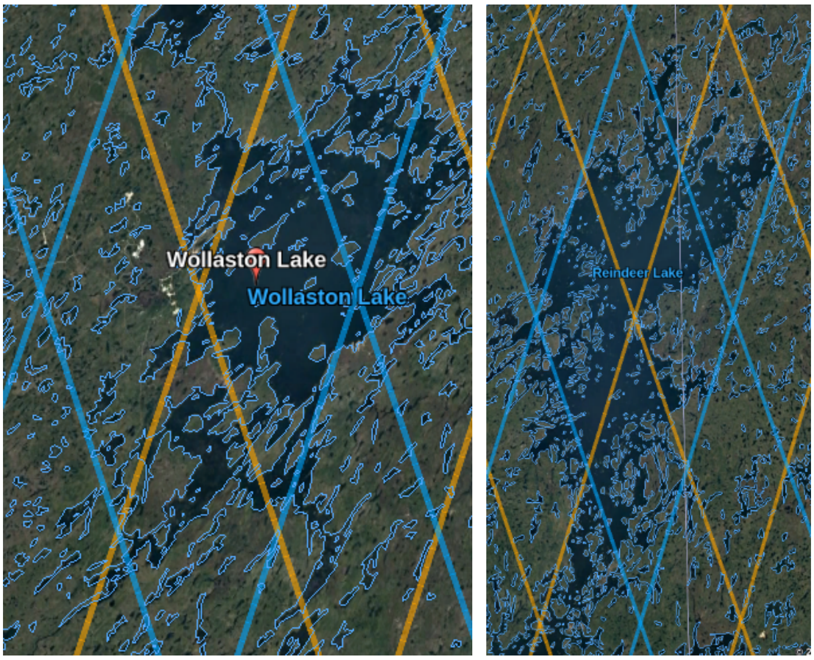

Figure 3.10.1 Wollaston and Reindeer Lakes. The location of the S3A (blue) and S3B (orange) reference tracks are also shown.

4 Validation of new DTC and WTC over CZ and IW regions (UPorto)

This section describes the set of procedures conducted by UPorto to assess the Dry Tropospheric Correction (DTC) and the Wet Tropospheric Correction (WTC) developed in WP2200 of the HYDROCOASTAL project.

This refers to the assessment performed by UPorto in the three selected test areas (Caspian Sea, Danube River and Java Sea). Additional independent validation of the corrections shall also be performed by other partners (in WP2500) in all test areas.

As the corrections are computed using an integrated approach, i.e., continuous corrections over all surface types (including ocean, coastal and inland water regions), a single validation plan is proposed.

Analyses will be performed both globally (for all test areas) and separately for the three selected areas: Caspian Sea, Danube River and Java Sea

4.1 Validation of the WTC

In this task, well established methodologies for the assessment of WTC datasets (Fernandes and Lázaro, 2016, 2018) will be adopted in the validation of the new WTC, namely:

a) Comparison with the MWR-derived WTC present in products (only for S3) – for coastal regions and large lakes (Caspian and Java Seas).
b) Comparison with the WTC from the ECMWF operational model – for all regions.
c) Comparison with independent WTC from MWR on board the reference missions and from imaging sensors such as the Global Precipitation Measurement (GPM) Microwave Imager (GMI) - over coastal regions and large lakes (Caspian and Java Seas).
d) Comparison with GNSS-derived WTC – this will provide information mainly about algorithm performance in the coastal regions and over IW regions with abundant number of GNSS stations.
e) Sea/water level anomaly variance analysis, along track, at crossovers, function of distance from coast or from lake-border, and function of latitude.
f) Error analysis based on the formal error, an additional output of the GPD+ algorithm.

4.2 Validation of the DTC

Since most errors associated with the DTC are systematic, validation diagnostics such as water level variance analysis are not appropriate. The following analysis shall be performed:

1. Along-track analysis of DTC and water level profiles, inspecting unexpected behaviour of the correction, present in some current products
2. Comparison with DTC present in products and with DTC derived from in situ pressure data, where available.

5 References

Aldarias, A., Gómez-Enri, J., Laiz, I., Tejedor, B., Vignudelli, S., Cipollini, P. Validation of Sentinel-3A SRAL Coastal Sea Level Data at High Posting Rate: 80 Hz. IEEE Transactions on Geoscience and Remote Sensing, 58, 6, 3809-3821. doi: 10.1109/TGRS.2019.2957649. 2020.

Andersen, O. B., Nielsen, K., Knudsen, P., Hughes, C. W., Bingham, R., Fenoglio-Marc, L., Gravelle, M., Kern, M., & Polo, S. P. (2018). Improving the coastal mean dynamic topography by geodetic combination of tide gauge and satellite altimetry. Marine Geodesy, 41(6), 517–545. https://doi.org/10.1080/01490419.2018.1530320.

Berghuijs W. R., Sivapalan M., Woods R. A., Savenije H. G. (2014). “Patterns of similarity of seasonal water balances: A window into streamflow variability over a range of time scales”. Water Resources Research, vol. 50, num 7, p. 5638-5661, doi:10.1002/2014WR015692.

Bouffard, J., Naeije, M., Banks, C.J., Calafat, F.M., Cipollini, P., Snaith, H.M., Webb, E., Hall, A., Mannan, R., Féménias, P. and Parrinello, T., 2018. CryoSat ocean product quality status and future evolution. *Advances in Space Research*, *62*(6), pp.1549-1563.

Bryden, H. L. Kinder, T. H. Steady two-layer exchange through the Strait of Gibraltar, Deep-Sea Research., doi: 10.1016/S0198-0149(12)80020-3. 1991.

Busker T., de Roo A., Gelati E., Schwatke C., Adamovic M., Bisselink B., Pekel J.-F., Cottam A.: A global lake and reservoir volume analysis using a surface water dataset and satellite altimetry. Hydrology and Earth System Sciences, 23(2), 669-690, 10.5194/hess-23-669-2019, 2019

Calafat, F. M., P. Cipollini, J. Bouffard, H. Snaith, P. Féménias. Evaluation of new CryoSat-2 products over the ocean, Remote Sens. Environ., 191, 131-144, 2017.

Cipollini, P. (2011). A new parameter to facilitate screening of coastal altimetry data and corrections. Presented at the 5th Coastal Altimetry Workshop, San Diego, USA available from http://www.coastalt.eu/sites/default/files/sandiegoworkshop11/poster/P08_Cipollini_Castal_Proximity.pdf

Criado-Aldeanueva, F., García-Lafuente, J., Navarro, G., Ruiz, J. Seasonal and interannual variability of the surface circulation in the eastern Gulf of Cadiz (SW Iberia). Journal of Geophysical Research: Oceans, 114(C1). doi: 10.1029/2008JC005069. 2009.

Dinardo S., Fenoglio-Marc L., Buchhaupt C., Becker M., Scharro R., Fernandez J. Benveniste J. (2018). CryoSat-2 performance along the German coasts, AdSR special Issue CryoSat-2, https://doi.org/10.1016/j.asr.2017.12.018

Dinardo S., Fenoglio L., M. Becker; R. Scharroo; M. J. Fernandes; J. Staneva; S. Grayek; J. Benveniste (2020), A RIP-based SAR Retracker and its application in North East Atlantic with Sentinel-3, Advances in Space Research (2020), doi: https://doi.org/10.1016/j.asr.2020.06.004

Dinardo, S., 2020. Techniques and applications for Satellite SAR Altimetry over water, land and ice. PhD Dissertation Thesis. 56, Darmstadt, Germany, Technische Universität Darmstadt, ISBN 978-3-935631-45-7. https://doi.org/10.25534/tuprints-00011343.

Fabry P., Bercher N., Roca M., Martinez B., Fernandes J., Lázaro C., Gustafsson D., Arheimer B., Ambrózio A, Restano M, Benveniste J. (2016). "A step towards the characterization of SAR Mode Altimetry Data over Inland Waters – SHAPE Project". In “New era of altimetry, new challenges”, Ocean Surface Topography Science Team meeting (OSTST), 31 Oct – 4 Nov 2016, La Rochelle, France

Fabry, P. and Bercher, N. (2015). “Characterization of SAR Mode Altimetry over Inland Water”. In Proceedings of the Sentinel-3 for Science Workshop, 2-6 June, Venice, Italy

Fenoglio-Marc, L., Dinardo, S., Scharroo, R., Roland, A., Dutour, M., Lucas, B., Becker, M., Benveniste, J., Weiss, R. (2015): The German Bight: a validation of CryoSat-2 altimeter data in SAR mode, Adv. Space Res., doi: 10.1016/j.asr.2015.02.014

Fenoglio-Marc, L., Dinardo, S., Buchhaupt, C., Scharroo, R., Becker, M., and Benveniste, J. (2019). Calibrating the SAR Sea Surface Heights of CryoSat-2 and Sentinel-3 along the German coasts. In Proceedings of International Association of Geodesy Symposia

Fenoglio L., S. Dinardo, B. Uebbing, C. Buchhaupt, M. Gärtner, J. Staneva, M. Becker, A. Klose, J. Kusche, M. Becker. Investigating improved coastal Sea Level Change from Delay Doppler Altimetry in the North-Eastern Atlantic, Adv. Space Res., under review

Fernandes, M. J., Lázaro, C. (2016). GPD+ Wet Tropospheric Corrections for CryoSat-2 and GFO Altimetry Missions. Remote Sensing, 8(10), 851. doi:10.3390/rs8100851

Fernandes, M. J., Lázaro, C. (2018). Independent assessment of Sentinel-3A wet tropospheric correction over the open and coastal ocean. (2018) Remote Sensing, 10(3), 484. doi:10.3390/rs10030484

Fukumori, I., Menemenlis, D. Lee, T. A near-uniform basin-wide sea level fluctuation of the Mediterranean Sea. Journal of Physical Oceanography. doi: 10.1175/JPO3016.1. 2007.

García-Lafuente, J., Delgado, J., Criado-Aldeanueva, F., Bruno, M., del Río, J., Vargas, J. M. Water mass circulation on the continental shelf of the Gulf of Cadiz. Deep Sea Research Part II: Topical Studies in Oceanography, 53(11-13), 1182-1197. doi: 10.1016/j.dsr2.2006.04.011. 2006.

Garel, E., Laiz, I., Drago, T., Relvas, P. Characterisation of coastal counter-currents on the inner shelf of the Gulf of Cadiz. Journal of Marine Systems, 155, 19-34. doi: 10.1016/j.jmarsys.2015.11.001. 2016.

Gómez-Enri, J., Aboitiz, A., Tejedor, B., Villares, P. Seasonal and interannual variability in the Gulf of Cadiz: Validation of gridded altimeter products. Estuarine, Coastal and Shelf Science 96, 114-121. doi: 10.1016/j.ecss.2011.10.013. 2012.

Gómez-Enri, J., Escudier, R., Pascual, A., Mañanes, R. Heavy Guadalquivir River discharge detection with satellite altimetry: The case of the Eastern continental shelf of the Gulf of Cadiz (Iberian Peninsula). Advances in Space Research. DOI: 10.1016/j.asr.2014.12.039. 2015.

Gómez-Enri, J., P. Cipollini, M. Passaro, S. Vignudelli, B. Tejedor, J. Coca. Coastal altimetry products in the Strait of Gibraltar. IEEE Transactions on Geoscience and Remote Sensing. 54, 5455-5466. doi: 10.1109/TGRS.2016.2565472. 2016.

Gómez-Enri, J., Vignudelli, S., Cipollini, P., Coca, J., González, C.J. Validation of CryoSat-2 SIRAL sea level data in the eastern continental shelf of the Gulf of Cadiz (Spain). Advances in Space Research. doi: 10.1016/j.asr.2017.10.042. 2018.

Gómez-Enri, J., González, C.J. Passaro, M., Vignudelli, S. Álvarez, O., Cipollini, P., Mañanes, R., Bruno, M., López-Carmona, M.P., Izquierdo, A. Wind-induced cross-strait sea level variability in the Strait of Gibraltar from coastal altimetry and in-situ measurements. Remote Sensing of Environment, 221, 596-608. doi: 10.1016/j.rse.2018.11.042. 2019.

Gupta, Hoshin & Kling, Harald & Yilmaz, Koray & Martinez, Guillermo. (2009). Decomposition of the Mean Squared Error and NSE Performance Criteria: Implications for Improving Hydrological Modelling. Journal of Hydrology. 377. 80-91. 10.1016/j.jhydrol.2009.08.003.

Jiang, L., Nielsen, K., Andersen, O. B., Bauer-Gottwein, P. CryoSat-2 radar altimetry for monitoring freshwater resources of China. Remote Sensing of Environment, 200, 125-139. doi: 10.1016/j.rse.2017.08.015. 2017

Jiang, L., Madsen, H., Bauer-Gottwein, P. Simultaneous calibration of multiple hydrodynamic model parameters using satellite altimetry observations of water surface elevation in the Songhua River. Remote Sensing of Environment, 225, 229-247. doi: 10.1016/j.rse.2019.03.014. 2019

Jiang, L., Nielsen, K., Dinardo, S., Andersen, O. B., Bauer-Gottwein, P. Evaluation of Sentinel-3 SRAL SAR altimetry over Chinese rivers. Remote Sensing of Environment, 237, 111546. doi: 10.1016/j.rse.2019.111546. 2020

Kittel, C. M. M., Jiang, L., Tøttrup, C., Bauer-Gottwein P. Sentinel-3 radar altimetry for river monitoring – a catchment-scale evaluation of satellite water surface elevation from Sentinel-3A and Sentinel-3B. Hydrol. Earth Syst. Sci. Discuss., https://doi.org/10.5194/hess-2020-165, 2020. Preprint under review for HESS

Kosuth P., Blitzkow D., Cochonneau G. (2006). "Establishment of an altimetric reference network over the Amazon basin using satellite radar altimetry (Topex/Poseidon)", in the proceedings of the "15 years of progress in radar altimetry" Symposium, Venice, Italy.

Kouraev A.V., Zakharova E.A., Samain O., Mognard-Campbell N., Cazenave A. "Ob' river discharge from TOPEX/Poseidon satellite altimetry data". Remote Sensing of Environment, 93, 2004, pp. 238-245

Lacombe, H. Richez, C. The regime in the Strait of Gibraltar. In Hydrodynamics of Semi-Enclosed Seas, Jacques C.J. Nihoul (ed.), ISBN: 978-0-444-42077-0, 13-73. 1982.

Laiz, I., Gómez-Enri, J., Tejedor, B., Aboitiz, A., Villares, P. Seasonal sea level variations in the gulf of Cadiz continental shelf from in-situ measurements and satellite altimetry. Continental Shelf Research 53, 77-88. doi: 10.1016/j.csr.2012.12.008. 2013.

Menemenlis, D. Fukumori, I. Lee, T. Atlantic to Mediterranean Sea Level Difference Driven by Winds near Gibraltar Strait. Journal of Physical Oceanography. doi: 10.1175/JPO3015.1. 2007.

Nash J.E., Sutcliffe J.V. (1970). "River flow forecasting through conceptual models part I — A discussion of principles", Journal of Hydrology, Volume 10,iIssue 3, p. 282-290, ISSN 0022-1694, doi:10.1016/0022-1694(70)90255-6.

Passaro, M., P. Cipollini, S. Vignudelli, G. Quartly, and H. Snaith, (2014) "ALES: A multi-mission subwaveform retracker for coastal and open ocean altimetry", Remote Sensing of the Environment, vol. 145, pp. 173-189, 2014.

Passaro, M., Dinardo, S., Quartly, G.D., Snaith, H.N., Benveniste, J., Cipollini, P., Lucas, B. Cross-calibrating ALES Envisat and CryoSat-2 Delay-Doppler: a coastal altimetry study in the Indonesian Seas. Adv. Space Res. 58, 289–303. doi: 10.1016/j.asr.2016.04.011. 2016.

Passaro M., Rose S.K., Andersen O.B., Boergens E., Calafat F.M., Dettmering D., Benveniste J.: ALES+: Adapting a homogenous ocean retracker for satellite altimetry to sea ice leads, coastal and inland waters. Remote Sensing of Environment, 211, 456-471, 10.1016/j.rse.2018.02.074, 2018.

Pawlowicz, R., Beardsley, B., & Lentz, S. Classical tidal harmonic analysis including error estimates in MATLAB using T_TIDE. Computers & Geosciences, 28(8), 929-937. 2002.

Peliz, A., Dubert, J., Marchesiello, P., Teles-Machado, A. Surface circulation in the Gulf of Cadiz: Model and mean flow structure. Journal of Geophysical Research-Oceans 112. doi: 10.1029/2007JC004159. 2007

Relvas, P., Barton, E. D. Mesoscale patterns in the Cape Sao Vicente (Iberian peninsula) upwelling region. Journal of Geophysical Research: Oceans, 107(C10), 28-1. doi: 10.1029/2000JC000456. 2002.

Schwatke C., Dettmering D., Bosch W., Seitz F.: DAHITI – an innovative approach for estimating water level time series over inland waters using multi-mission satellite altimetry. Hydrology and Earth System Sciences 19(10): 4345-4364, 10.5194/hess-19-4345-2015, 2015

Schwatke C., Scherer D., Dettmering D.: Automated Extraction of Consistent Time-Variable Water Surfaces of Lakes and Reservoirs Based on Landsat and Sentinel-2. Remote Sensing, 11(9), 1010, 10.3390/rs11091010, 2019

Schwatke C., Dettmering D., Seitz F.: Volume Variations of Small Inland Water Bodies from a Combination of Satellite Altimetry and Optical Imagery. Remote Sensing, 12(10), 1606, 10.3390/rs12101606, 2020

Stevenson, R.E. Huelva Front and Malaga, Spain, Eddy chain as defined by satellite and oceanographic data. Deutsche Hydrographische Zeitschrift 30 (2), 51–53. doi: 10.1007/BF02226082. 1977.

Zakharova EA., Nielsen K., Kamenev G., Kouraev A., River discharge estimation from radar altimetry: Assessment of satellite performance, river scales and methods, Journal of Hydrology, 2020, 583, 124561.

List of Acronyms

ACE2 Altimeter Corrected Elevations (vers. 2)
AD Applicable Documents
AGC Automatic Gain Control
AH Alti-Hydro
AHP Alti-Hydro Product(s)
AI Action Item
AIM Action Item Management (tool)
AltiKa Altimeter in Ka band and bi-frequency radiometer instrument
AMSR-E Advanced Microwave Scanning Radiometer-Earth Observing System
ANA Agência Nacional de Águas (National Water Agency, Brazil)
AoA Angle of arrival
API Application Programming Interface
AR Acceptance Review
ASAP As Soon As Possible
ASCII American Standard Code for Information Interchange
ATBD Algorithm Technical Basis Document
ATK ALONG-TRACK S.A.S.
AVISO Archivage, Validation et Interprétation des données des Satellites Océanographiques
BfG German Federal Institute of Hydrology
BKG German Federal Agency for Cartography and Geodesy
BSH German Federal Maritime and Hydrographic Agency
BIPR Background Intellectual Property Right
CASH Contribution de l'Altimetrie Spatiale à l'Hydrologie (Contribution of Space Altimetry to Hydrology)
CCN Contract Change Notice
CFI Customer Furnished Item
CLASS NOAA/Comprehensive Large Array-Data Stewardship System
CoG Centre of Gravity
CNES Centre Nationales des Etudes Spatiales
CPP CryoSat-2 Processing Prototype (CNES)
CryoSat-2 Altimetry satellite for the measurement of the polar ice caps and the ice thickness
CRISTAL Copernicus polaR Ice and Snow Topography ALtimeter
CRUCIAL CRyosat-2 sUCcess over Inland wAter and Land
CSV Coma Separated Values
CTOH Centre de Topographie des Océans et de l'Hydrosphère (Centre of Topography of the Oceans and the Hydrosphere)
DAC Dynamic Atmospheric Correction
DAHITI Database for Hydrological Time Series of Inland Waters
DAO Data Access Object
DARD Data Access Requirement Document
DDM Delay-Doppler Map
DDP Delay-Doppler Processor
DEM Digital Elevation Model
DGC Doppler Ground Cell
DPM Detailed Processing Model
DPP Data Procurement Plan
DTC Dry Tropospheric Correction
DTU Danmarks Tekniske Universitet (Technical University of Denmark)
DVT Data Validation Table
ECMWF European Centre for Medium-Range Weather Forecasts
ECSS European Cooperation for Space Standardisation
EGM Earth Gravitational Model
ENVISAT ENVIronment SATellite
EO Earth Observation
EOEP Earth Observation Enveloppe Programme
EOLi Earth Observation Link
EOLi-SA EOLi-Stand Alone
EPN EUREF Permanent Network
ERA Iterim ECMWF ReAnalysis
ESA European Space Agency
EUREF IAG Reference Frame Sub-Commission for Europe
FBR Full Bit Rate
FFT Fast Fourier Transform
FR Final Review

FTP File Transfer Protocol

FCUP (from portuguese) *“Faculdade de Ciências da Universidade”*, Science faculty of the University of Porto

GDAL Geospatial Data Abstraction Library

GDR, [I-,S-] Geophysical Data Record, [Interim-, Scientific-]

GFZ Deutsche GeoForschungsZentrum (German Research Centre for Geosciences)

GIM Global Ionospheric Maps

GLOSS Global Sea Level Observing System

GNSS Global Navigation Satellite System

GOCE Gravity field and steady-state Ocean Circulation Explorer

GPD GNSS-derived Path Delay

G-POD Grid Processing on Demand

GPT2 Global Pressure and Temperature model (vers. 2)

GPP Ground Processing Processor

GPS Global Positioning System

GRACE Gravity Recovery And Climate Experiment

GRDC Global Runoff Data Centre

GRGS Groupe de Recherche de Géodésie Spatiale (Space Geodesy Research Group)

GRLM Global Reservoir and Lake Monitor

GSHHS Global Self-consistent, Hierarchical, High-resolution Shorelines

GTN-L Global Terrestrial Network - Lakes

HDF-EOS Hierarchical Data Format - Earth Observing System

HGT A SRTM file format

HWS High Water Stage

HYCOS Hycos Hydraulics & Control Systems

HYPE Hydrological Predictions for the Environment model

IAG International Association of Geodesy

IDAN Intensity-Driven Adaptive-Neighbourhood

IE Individual Echoes

IGS International GNSS (Global Navigation Satellite Systems) Service

IM Internal Meeting (e.g. not with the client)

IODD Input Output Data Document

IPF Integrated Processing Facility

ISD isardSAT

ITRF International Terrestrial Reference Frame

IRF Impulse Response Function

Jason-1 Altimetry satellite, T/P follow-on

Jason-2 Altimetry satellite, also knwon as the « Ocean Surface Topography Mission » (OSTM), Jason-1 follow-on

Jason-3 Altimetry satellite, Jason-2 follow-on

Jason-CS Jason Continuity of Service

KGE Kling-Gupta efficiency

KML Keyhole Markup Language

KO Kick Off

L1A Level-1A

L1B Level-1B

L1B-S, L1BS Level-1B-S (aka, Stack data)

L2 Level-2

L3 Level-3

L4 Level-4

LAGEOS Laser Geodynamics Satellite

LEGOS (french acr.) Laboratoire d'Études en Géophysique et Océanographie Spatiale (Laboratory for Studies in Geophysics and Spatial Oceanography)

LOTUS Preparing Land and Ocean Take Up from Sentinel-3

LPS Living Planet Symposium

LRM Low Resolution Mode

LSE Least Square Estimator

LWL Lake Water Level

LWS Low Water Stage

MARS Meteorological Archival and Retrieval System

MDL Minimum Description Length

MMSE Minimum Mean Square Error

MNDWI Modification of Normalised Difference Water Index

MoM Minutes of Meeting

MPC Mission Performance Centre

MRC Mekong River Commission

MTR Mid Term Review

MSS Mean Square Slope

MSS Mean Sea Surface

MWR Microwave Radiometer

NAVATT Navigation and Attitude

NDBC US National Data Buoy Center

NDVI Normalised Difference Vegetation Index

NDWI Normalised Difference Water Index

netCDF Network Common Data Form

NOAA National Oceanic and Atmospheric Administration

NR New Requirement (w.r.t. the SoW)

NRT Near Real-Time

NSE Nash-Sutcliffe model efficiency coefficient

NWM Numerical Weather Model

OCOG Offset Centre of Gravity

OPC One per Crossing

OSTM Ocean Surface Topography Mission (also known as Jason-2), is also the name of the satellites series T/P, Jason-1, Jason-2 and Jason-3

OVS Orbit State Vector

PDF Probability Density Function

PEACHI Prototype for Expertise on AltiKa for Coastal, Hydrology and Ice

PEPS Sentinel Product Exploitation Platform (CNES)

PISTACH (french acr.) Prototype Innovant de Système de Traitement pour les Applications Cotières et l'Hydrologie

PLRM Pseudo Low Rate Mode

PMP Project Management Plan

POCCD Processing Options Configuration Control Document

PR Progress Report

PRF Pulse Repetition Frequency

PSD Product Specification Document

PSMSL Permanent Service for Mean Seal Level

PTR Point Target Response

PVP Product Validation Plan

PVR Product Validation Report

PVS Pseudo Virtual Station(s)

RADS Radar Altimeter Database System

RB Requirements Baseline (document)

RCMC Range Cell Migration Curve

RCS Radar Cross Section

RD Reference Document

RDSAR Reduced SAR (also known as Pseudo-LRM)

RF Random Forest

RGB Red, Green, Blue

RID Review Item Discrepancy

RIP Range Integrated Power (of the MLD) sometimes referred as Angular Power Response (APR)

RMS Root Mean Square

rmse root mean square error

ROI (geographical) Region(s) Of Interest

RP Report Period (a month that is being reported into a Progress Report)

RSS Remote Sensing Systems

RWD River Water Discharge

RWL River Water Level

SAMOSA SAR Altimetry MOde Studies and Applications

SARAL In Indian "simple", in english "SAtellite for ARgos and AltiKa.

SARIn SAR Interferometric (CryoSat-2/SIRAL mode)

SAR Synthetic Aperture Radar

SARvatore SAR Versatile Altimetric Toolkit for Ocean Research & Exploitation

SCOOP SAR Altimetry Coastal & Open Ocean Performance

SDP Software Development Plan

SEOM Scientific Exploitation of Operational Missions

SHAPE Sentinel-3 Hydrologic Altimetry PrototypE

SI-MWR Scanning Imaging MWR

SLA Sea Level Anomaly

SLR Sampling Loss Rate

SME Small and Medium-sized Enterprise

SMHI Swedish Meteorological and Hydrological Institute

SNAP SeNtinel Application Platform

SOA State Of the Art

SONEL Système d'Obserbvations du Niveau des Eaux Littorales

SOW Statement Of Work

SPR Software Problem Reporting

SPS Sentinel-3 Surface Topography Mission System Performance Simulator

SRAL SAR Radar Altimeter

SRTM Shuttle Radar Topography Mission

SSB Sea State Bias

SSH Sea Surface Height

SSMI/IS Special Sensor Microwave Imager (SSM/I) Sounder

SSO Single Sign-On

Stack Matrix of stacked Doppler beams

STD Standard Deviation

STDD Standard Deviation of Differences

STM Sentinel-3 Surface Topography Mission

SUM Software User Manual
SWBD SRTM Water Body Data
SWH Significant Wave Height
TAI Temps Atomique International (International Atomic Time)
TBC To Be Confirmed
TBD To Be Done
TCWV Total Column Water Vapour
TDS Test Data Set
TMI Tropical Rainfall Measuring Mission (TRMM) Microwave Imager
TN Technical Note
T/P Topex/Poseidon (altimetry satellite)
TR Technical Risk
UNESCO United Nations Educational, Scientific and Cultural Organization
URL Uniform Resource Locator
USGS United States Geological Survey
USO Ultra Stable Oscillator
USSH Uncorrected Sea Surface Height
UTC Coordinated Universal Time
UWM Updated Water Mask
VS Virtual Station(s)
VH Vertical-Horizontal polarisation
VV Vertical-Vertical polarisation
WBS Work Breakdown Structure
WFR Water Fraction Ratio
WFRWF Water Fraction Ratio - Water content in Footprint
WMO World Meteorological Organization
WP Work Package(s)
w.r.t. with respect to
WTC Wet Tropospheric Correction
XML eXtensible Markup Language
ZP Zero Padding